IEEE P802.15
Wireless Personal Area Networks

Project	IEEE P802.15 Working Group for Wireless Personal Area Networks (WPANs)		
Title	**UWB Channel Model for under 1 GHz (VHF and UHF)**		
Date Submitted	[12 September 2004] [rev4: 13 Nov 2004]		
Source	[Kai Siwiak] [TimeDerivative] [Coral Springs, FL]	Voice: Fax: E-mail:	[+1 954-937-3288] [ ] [k.siwiak@ieee.org]
Re:	Adjunct to TG4a channel model document.		
Abstract	This paper presents a channel model for UWB pulse systems operating at VHF and UHF.		
Purpose	The purpose of this document is to provide IEEE P802.15 with a VHF-UHF channel model for evaluating location aware wireless systems.		
Notice	This document has been prepared to assist the IEEE P802.15. It is offered as a basis for discussion and is not binding on the contributing individual(s) or organization(s). The material in this document is subject to change in form and content after further study. The contributor(s) reserve(s) the right to add, amend or withdraw material contained herein.		
Release	The contributor acknowledges and accepts that this contribution becomes the property of IEEE and may be made publicly available by P802.15.		

Revision History

Preliminary Draft	10 Sep 2004.
r0	12 Oct 2004.
r1	18 Oct 2004. Improved descriptions and detailed write-up.
r2	27 Oct 2004. Modifications recommended by the TG4a channel model committee. (i) "For the LOS case, each of the deterministic rays is seen as the center of a cluster; each cluster having several components." ***The wall reflections were modified to add delayed reflection component due to transmission through, and reflection from the other side of the wall. The result is a single additional term for each primary wall reflection. Thus all energy terms up to about 30 dB below the direct component are included.*** (ii) "The amplitude distribution of the fading of the clusters has to be specified." ***The added fading clusters are deterministic. They are based on an additional reflection from the back side of a wall. An additional wall thickness parameter with an initial value of 12 cm has been added.*** (iii) "Measurement results, especially the model of Cassioli et al., should be used as much as possible to parameterize the model. Room dimensions should be chosen such that the resulting impulse responses agree reasonably well with those measurement results." ***The room parameters are a model input. The dimensions chosen match the delay characteristics in Cassioli et al., for the distances involved.*** (iv) "Pathloss exponent and attenuation at 1m distance needs to be included." ***The path loss exponent is already a part of the model since the preliminary draft. Spherical wave propagation is assumed for all paths (path loss exponent is thus 2) as seen in Equation (24). Path amplitudes are deterministically attenuated additionally by wall reflections and transmissions.*** (v) "The delay spread should be independent of the distance." ***The distance dependency of delay spread is critical to the overall attenuation of components in NLOS conditions and is seen in*** **[Yano 2002], [IEEE802 02/282]** ***and*** **[DaSilva 2003].** ***It is relevant to how energy can be gathered by a receiver employing rake or channel equalization. Representative distances can be selected as desired.***
r3	Modified multipath Equations.
r4	**a)** 100 realizations of the channel model case-1 and case-2 generated; package containing the realizations included. **b)** Added antenna efficiency and body-proximate coupling effects.

15-04-0505-00-004a-UWB Channel Model for VHF and UHF

Introduction

A channel model has been tailored for use in the VHF and UHF frequency range. The special needs of ultra-wide band impulses and impulse doublets in this range are met by a line of sight model which deterministic imaging methodology to calculate 13 strongest multipath reflections within a room. Only wall reflections are considered, in so far as the wavelengths under consideration approach several meters. This LOS model brings into play a severe multipath distortion phenomenon based on the strict correlation imposed by the wall boundary conditions between the multipath components. In other words, in LOS case, the multipath is not stochastic the multipath components are correlated, and *the model can be used for studying the case of motion between the transmitter and receiver*. The total energy received in the room exceeds the direct path energy even though spherical wave propagation is imposed on all paths. This effect has often been "curve fit" in other models by an unrealistically smaller than 2 propagation coefficient. The misuse of such results and misapplication to interference studies is causing havoc at forums like the ITU-R TG1-8 on UWB. The RMS delay spread of the multipath within a room was seen to be a linear function of the room dimensions.

A non-line of sight extension to the VHF-UHF channel model uses a stochastic method to generate exponentially weighted multipath components for which the delay spread increases with distance, as is seen in measurement of both UWB impulses and of narrow band signals. The resulting multipath model *at any range* can be derived from a common set of randomly generated trials by a simple scaling formula of the model. The increase of RMS delay spread with distance is one of the reasons why the apparent power law of propagation higher than 2 in scattering environments. The model correctly scales this effect, and thus models realistic energy per component versus distance. A Ricean parameter allows the total energy in the NLOS case to be divided between a direct path component and diffuse multipath energy.

Finally, the antenna efficiency and antenna pattern distortion due to the body proximity effect are captured in an antenna efficiency term of the model. It is pointed out, and referenced extensively, that a properly designed antenna close to the human body looks like a lossy wire antenna having the body longitudinal dimensions. The effect enhances link margin in the VHF and lower UHF frequencies, but begins to exhibit a deep pattern null at the upper VHF and the UHF frequencies.

The VHF-UHF channel model was designed with a direct physical interpretation for impulses and impulse doublets for simplicity. Guidance is provided for antenna patterns and antenna efficiency for body mounted devices, particularly for use below 300 MHz. There is no channel model in the current literature that applies to impulse doublets which spread energy over a 200% bandwidth in that range. This model comprises two cases, and includes 100 realizations of each of the two cases of channel model.

The **first model case** is a *deterministic* line of sight (LOS) in-room model that captures the major reflection sources at low frequencies. These reflections are the room walls and floor for the

LOS case. All components to about 30 dB below the direct component are captured. The computed RMS delay spread is found to be a linear function of room dimensions. Fourteen deterministic paths are included. Deterministic models are not unprecedented [Canada 2004]; they can provide a mechanism for studying impulse and pulse distortions. The transmitter and receiver 3-dimensional coordinates, channel model coefficients and delays are contained in a 100 row array (for the 100 realizations) in file: <15-04-0505-04-004a-los_1000MHz.txt> included in the package <15-04-0505-04-004a-UWB-Channel-Model-for-under-1-GHz.zip>.

The **second model case** is a non-line of sight (N-LOS) model based on the Jakes [Jakes 1974] model with exponential energy density profile (EDP). It includes a Ricean parameter K_F for splitting the energy between a direct an diffuse components. The multipath UWB pulses and impulses are exponentially distributed, their arrival interval is randomly distributed in windows of duration T_m. The delay spread increases with distance but the total energy is constant, as is observed in experiment, thus a physically realistic propagation law naturally evolves from the model. Data files from which 100 realizations of the channel model can be constructed at *any desired distance* are contained in the two data file:

<15-04-0505-04-004a-NLOS_1000MHz_HK.txt>
<15-04-0505-04-004a-NLOS_1000MHz_TM.txt>

The first data file contains an array of channel coefficients corresponding to delays TM (normalized by T_m) contained in the corresponding delay time array.

For both the LOS and NLOS cases a signal $S(t)$ contains all of the multipath components, weighted by the receiver antenna aperture A_e, and by the receiver antenna efficiency $\eta_{ant.}$. The formulation of the multipath components, along with the time definition of UWB impulses, and the frequency dependent receiver antenna aperture and efficiency uniquely address the needs of a VHF-UHF impulse doublet. The method of signal detection, including the receiver filter and multiplication by the receiver template, and signal processing determine which, how many, and how efficiently the multipath components are utilized, and how accurately ranges are determined. The model evaluates UWB impulse radios in:

(1) direct free space propagation considering additive white Gaussian noise (AWGN),
(2) LOS conditions with multipath typical of a room, and with motion possible between transmitter and receiver, and
(3) a range on N-LOS conditions including direct and diffuse contributions and with delay spread a function of distance.

The model output is a signal profile in time which is the input to the UWB receiver. The full model code, rendered in Mathcad, is given in the Appendix of <15-04-0505-04-004a-sub-GHz-model.zip>.

Antennas in close proximity to the human body couple to the body, and depending on the polarization, type of antenna, and operating frequency range, may experience a significant field enhancement. An analysis is suggested, with the extensive details in the references.

Case 1: The Line of Sight Model

Impulse reflections and propagation, including coupling between antennas is discussed in [Siwiak 2004]. LOS attenuation is free space integral over PSD for distances: $d<(RoomX^2+RoomY^2)^{1/2}$ m
Where *RoomX* and *RoomY* are the room dimensions. Multipath is derived from a direct path and 13 primary reflections of a room model:

- 4 principal reflections from the walls (of order Γ_m = -5 dB)
- 1 ground reflection (of order $\cos(\theta)\Gamma_m$ = -7 dB)
- 4 principal corner reflections (of order Γ_m^2 = -10 dB)
- 4 secondary reflections from the walls (of order $(1+\Gamma_m)^2\Gamma_m$ = -21 dB)

The amplitude order estimates above do not include the additional differential distance path attenuation which is taken into account in the model. The next order reflection would include double internal wall bounces (-35 dB), and internal wall reflections involving a corner (-29+ dB). Thus, including path incremental increases, components up to 30 dB lower than the direct component are taken into account. Multiple realizations are utilized by randomly selecting a transmit and a receive point in the room. The selected points are no closer than d_t from any wall.

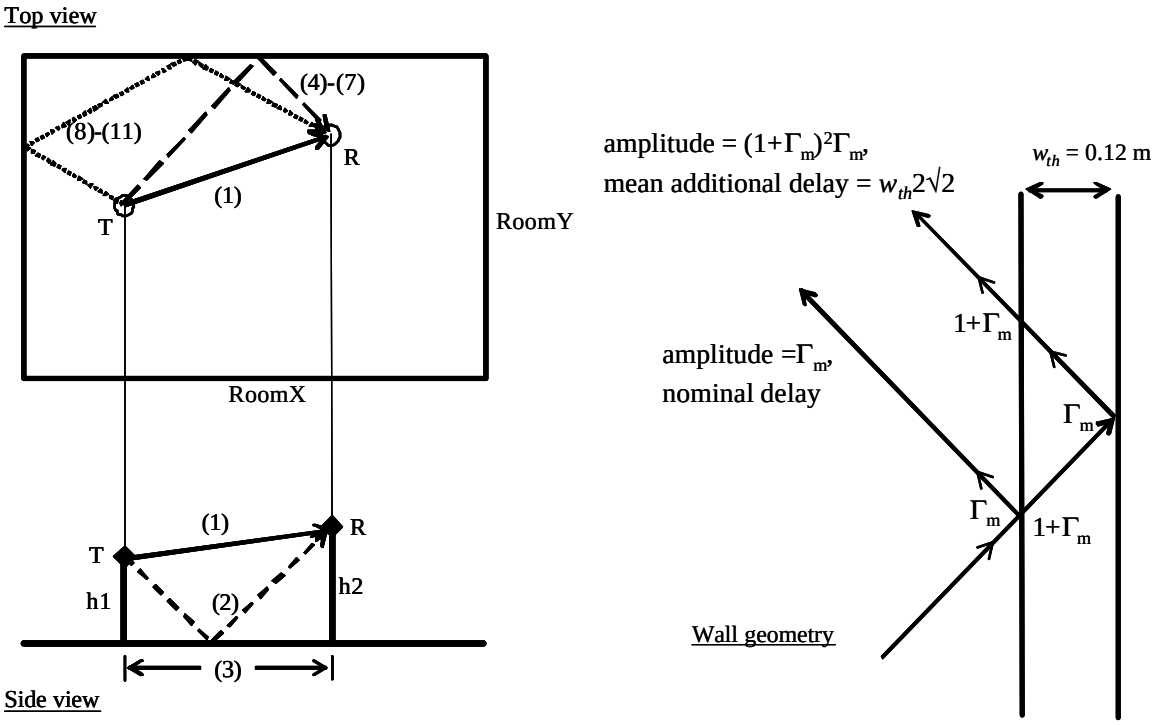

Figure 1. LOS components in a room of dimensions *RoomX* by *RoomY*. The wall secondary reflections are pictured on the right.

The LOS case of the channel model comprises 5 geometrical parameter and 3 signal parameters:

- Room dimensions *RoomX* and *RoomY*,
- Minimum distance to a wall *dt*,
- Wall thickness w_{th}
- Antenna height limits *h*1 and *h*2
- Average wall and floor reflection coefficient Γ_m
- Radiated power spectral density EIRPsd(*f*)
- Receiver antenna aperture A_e and antenna efficiency $\eta_{ant}(f)$

The reflection coefficient is derived from [Honch 1992]. Figure 1 shows the signal paths between a transmit antenna *T* and a receive antenna *R* in an LOS condition in the room. Total energy is accounted for in the room. The "excess" energy in the room should is balanced by the average wall-transmitted energy. The signals paths are:

- Direct path given by Equation (1),
- Ground (floor) reflection given by (2),
- Single wall reflections given by (4) through (7),
- Double wall reflections (corner bounces) given by (8) through (11)
- The effect of internal wall reflections is captured in Equations (16) through (18).

Secondary reflections which capture the main internal wall reflected energy, shown on the right side of Figure 1, are included. The derived parameters include:

- Multipath signal profile *S*(*t*)
- RMS delay spread τ_{rms},
- the mean ray arrival rate T_s
- excess energy factor in the room is W_x

The model operates by selecting at random multiple realizations (100 here) of random transmitter an receiver (*x, y, z*) coordinates bounded by the confines of the room (within d_t of the walls) and between antenna heights of h_1 and h_2. The one hundred realizations are depicted in Figure 2 of the Appendix in the package <15-04-0505-04-004a-UWB-Channel-Model-for-under-1-GHz.zip>.

The apparent total energy received at *R* is greater than would be obtained from a single path free space transmission from *T* because the reflections direct additional time dispersed signal copies to the receiver. It is important to note that the wave propagation along each path is governed by the physics of an expanding spherical wave, thus the energy in each path attenuates as the square of distance. The case resembles a Ricean distribution comprising significant energy in a direct path followed by a decaying multipath profile. On the average, in a 3.7 m by 4.6 m room, the energy in the multipath components is 2.2 dB below the direct path energy, thus the total available energy is 2 dB higher than contained in just the direct path. The statistics of the multipath components are nearly, but not quite described by a Rayleigh distribution.

Energy conservation dictates that the total energy leaving the room should equal the energy transmitted. This can be approximately checked by observing the product of the excess energy

factor with the average transmission coefficient $W_x[1 - \Gamma_m{}^2]$ which should be approximately one. The modeled case verifies this within approximately 0.13 dB.

The LOS model is specified by Equation (26), and supported by Equations (23), (24), and (25) in the Appendix. Specifically, the direct component and the multipath components are given by

$$\begin{aligned} H_{LOSi}(t) := {} & Vfs_i(d) + \left[\Gamma m \cdot \left(\frac{Dg_i}{Gr_i}\right) \cdot Vfs(d + eG) \cdot \delta\left(t - \frac{eG}{c}\right)\right] \quad ... \\ & + \left[\begin{array}{l} \Gamma m \cdot \left(\begin{array}{l} Vfs_i(d + eR1) \cdot \delta\left(t - \frac{eR1}{c}\right) \\ + Vfs_i(d + eR2) \cdot \delta\left(t - \frac{eR2}{c}\right) \\ + Vfs_i(d + eR3) \cdot \delta\left(t - \frac{eR3}{c}\right) \\ + Vfs_i(d + eR4) \cdot \delta\left(t - \frac{eR4}{c}\right) \end{array}\right) + \Gamma m^2 \cdot \left(\begin{array}{l} Vfs_i(d + eC1) \cdot \delta\left(t - \frac{eC1}{c}\right) \\ + Vfs_i(d + eC2) \cdot \delta\left(t - \frac{eC2}{c}\right) \\ + Vfs_i(d + eC3) \cdot \delta\left(t - \frac{eC3}{c}\right) \\ + Vfs_i(d + eC4) \cdot \delta\left(t - \frac{eC4}{c}\right) \end{array}\right) \\ + \Gamma m \cdot (1 + \Gamma m)^2 \cdot \left(\begin{array}{l} Vfs_i(d + eR1 + eW) \cdot \delta\left(t - \frac{eR1}{c} - \frac{eW}{c}\right) \\ + Vfs_i(d + eR2 + eW) \cdot \delta\left(t - \frac{eR2}{c} - \frac{eW}{c}\right) \\ + Vfs_i(d + eR3 + eW) \cdot \delta\left(t - \frac{eR3}{c} - \frac{eW}{c}\right) \\ + Vfs_i(d + eR4 + eW) \cdot \delta\left(t - \frac{eR4}{c} - \frac{eW}{c}\right) \end{array}\right) \end{array}\right] \end{aligned} \tag{23}$$

The component amplitude is given in terms of distance

$$Vfs(d) := \sqrt{\frac{\mu \cdot c}{4\pi}} \cdot \frac{1}{d} \tag{24}$$

The received energy is given in terms of a constant directivity antenna with efficiency $\eta_{ant}(f)$ and weighted by the emitted energy density profile EIRPsd(f)

$$Wrx := \frac{1.5}{4 \cdot \pi} \cdot \frac{1}{f_2 - f_1} \cdot \left[\int_{f_1}^{f_2} \left(\frac{c}{f}\right)^2 \cdot \eta_{ant}(f) \cdot EIRPsd(f)\, df\right] \tag{25}$$

Notice that Equation (25) explicitly takes into account the emitted field strength weighting of the receiver antenna aperture area, and that the receiver antenna efficiency is specifically taken into account. Finally, the received signal is

$$S(t) := H_{LOSi}(t) \cdot \sqrt{Wrx} \tag{26}$$

A data file, <15-04-0505-04-004-los_1000MHz.txt> attached to this package, has 100 realizations of the LOS model contained in a 32 column by 100 row array $WR_{r,c}$. Each row r contains one of the channel realizations where the column c values are:

X1, Y1, H1, X2, Y2, H2, A1, E1, A2, E2, ... A13, E13

Where one antenna is located at (X1, Y1, H1), the second antenna is located at (X2, Y2, H2) and the record of multipath amplitudes Ax and excess delays Ex, x=1 to 13, follow sequentially. The direct path *D* is the geometric distance between points (X1, Y1, H1) and (X2, Y2, H2). Equations (1) – (11), (13) and (14) can be used to calculated the geometric terms needed in Equation (23), however, the channel model can be reconstructed directly from the r by c data array WR using

$$H_{LOSi}(t) = Vfs(d) \left(\frac{d_i}{D_i} + \sum_{z=0}^{12} WR_{i,6+2z} \; \delta\left(t - WR_{i,7+2z}\right) \right) \tag{23a}$$

for the *i*-th channel realization. Here d_i is the antenna separation projected on the ground and D_i is the actual separation between antennas. The Mathcad code for the LOS model contains a rich set of test cases and illustrative plots showing the behavior of the various components. For example:

Figure 2 shows a random sampling of transmitter (red) and receiver (blue) locations within a room of dimensions *RoomX* and *RoomY*.

A parametric study using this model has revealed that the RMS delays spread scales linearly with the room dimensions. In fact, when the room dimensions are within an aspect ratio of less than about 3:1, a good approximation for the RMS delay spread in a room is

$$\tau_{RMS} = 0.2\ D/c$$

where *c* is the speed of propagation 299,792,458 m/s. Thus physical room size can be chosen to achieve a delay spread desired for the model study. In this case, the room dimensions chosen, 3.7 m by 4.6 m with a 1 m maximum antenna height differential, are typical of an office and giving a *D*=6 m which results in a 4 ns RMS delay spread and the mean propagation distance was 2.12 m. Other room dimensions may be chosen for other studies, however [DaSilva 2003] suggests that the chosen dimensions are adequate.

Figure 3 shows the images in the walls of the points shown in Figure 2. These image points are used to calculate the various reflection distances and differential delays.

Figure 4 shows the calculated energy profiles vs. differential delay for wall reflections involving the *RoomY* dimension of the room.

Figure 5 shows the calculated energy profiles vs. differential delay for wall reflections involving the *RoomX* dimension of the room. Since the room is not square, this EDP differs visibly from the one in Figure 4.

Figure 6 shows the EDP for the ground reflection. This energy component is closely related to the direct path energy, hence the profile has definite structure.

Figure 7 shows the EDP for the four corner reflections within the room.

Figure 8 is a depiction of the room and floor reflection coefficient.

Figures 9 and 10 compare an EDP sampling of wall and corner reflected energy and compares the points with an exponentially distributed profile having the same RMS delay spread.

Figure 11 shows EDPs for the four major paths: the black points are primary wall reflections, the red points correspond to corner reflections, the blue points are ground reflections, and the green points are wall reflection involving one internal wall bounce. There is a reasonable fit to the simple exponential distribution of the multipath, however, it must be realized that there is a specific deterministic relationship between the multipath component amplitudes and excess delays for any particular realization. The direct components has an amplitude of 1 and zero excess delay. Energy components as low as 40 dB below the direct signal are shown in this plot.

Figure 12 and 13 show one particular case of multipath: Figure 12 in the Appendix, and here, shows the reflection amplitudes, while Figure 13 shows the reflected component energies. Note that the multipath components can occur very close together, and they can be very far apart. On this scale the direct component has an amplitude of +1 and occurs at t=0.

Figure 14 (in the Appendix and here) shows a composite of a 100 of the LOS channel model impulse realizations. The red impulses are single wall reflections, hence the negative amplitudes. The green impulses are corner reflections which involve two reflections, hence the positive amplitudes. The black impulses represent ground reflected signals, and the magenta impulses are wall reflections that include two reflections internal to the wall. On this scale the direct component has an amplitude of +1 and occurs at t=0.

Figures 11 and 14 show the same impulse responses plotted on two different presentations. In each case it is apparent that there is a definite relationship among the four impulse components, as can be expected from a deterministic model. The behavior of the impulse responses is generally as noted in the measurements of Ghassemzadeh et al., in [IEEE802 04/504]. That is, the

first component is strongest followed by a nearly exponential decrease in the impulse components.

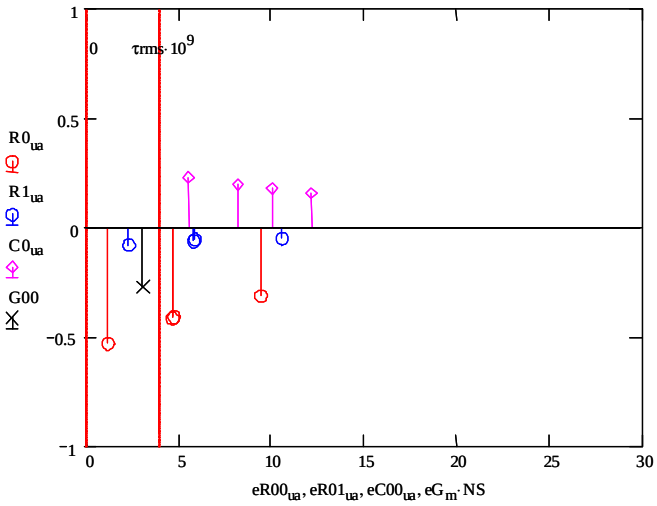

Figure 12. One particular realization of the LOS channel impulse amplitude response.

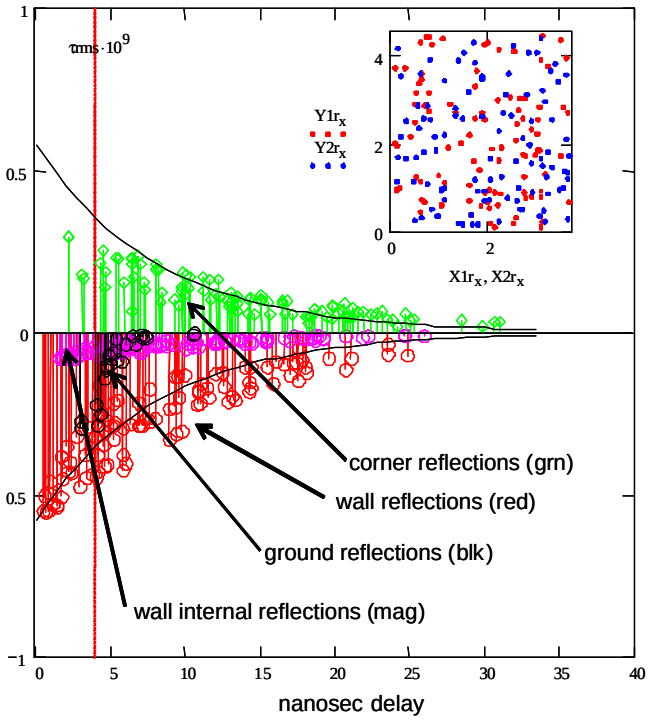

Figure 14. Hundred realizations of the LOS channel impulse amplitude responses.

Case-2: The Non-Line of Sight Multipath Model:

The non line of sight path is described by a modified Ricean EDP. This allows for parametric studies involving a direct component along with a diffuse component. Ranging errors can thus be studied with the fraction of direct path energy as a parameter. As such a total of 3 Ricean parameters plus an additional distance parameter totally specify the multipath profile. The multipath increases with distance, see [Siwiak 2003], and Ghassemzadeh et al., in [IEEE802 02/282], and [DaSilva 2003]. Here it is modeled by square root of distance d/D_t scaled by the constant τ_0. Energy dispersed into and increasingly longer multipath profile naturally results in an increase in the power law of propagation attenuation. Thus the increase by the square root of distance results in an overall inverse 2.5 power of distance for multipath components. Rather than a non-physical "phase parameter", a random distance variation within the mean interval T_m is used to define the time that multipath components arrive at the receiver. Total energy propagates as an expanding spherical wave, so the basic propagation is inverse square law, just like the LOS case. The unit energy is allocated a fraction K_F for the direct component, if any, and $(1-K_F)$ for the multipath energy.

The following parameters specific the UWB radio performance in a N-LOS condition:

- RMS delay spread parameter τ_0 s, and initial distance D_t
- Mean interval between rays T_m s
- Fraction of energy in direct component K_F
- Radiated power spectral density EIRPsd(f)
- Receiver antenna aperture A_e and antenna efficiency $\eta_{ant}(f)$

The channel model signal profile is

- Multipath signal amplitude profile $S_N(t)$

Figure 15 illustrates multiple realizations of the diffuse component of the channel impulse response for a case at a fixed distance of 5 m. An exponential delay envelope is superimposed for comparison.

Figure 16 illustrates multiple realizations of the diffuse component of the channel impulse response for a case at a fixed distance of 20 m. An exponential delay envelope is superimposed for comparison.

Figure 17 illustrates two specific realizations of the diffuse component of the channel impulse response, the upper one at a fixed distance of 5 m and the lower one at 20 m distance. An exponential delay envelope is superimposed for comparison.

Figure 15, 16 and 17 are in the APPENDIX, and reproduced here for convenience.

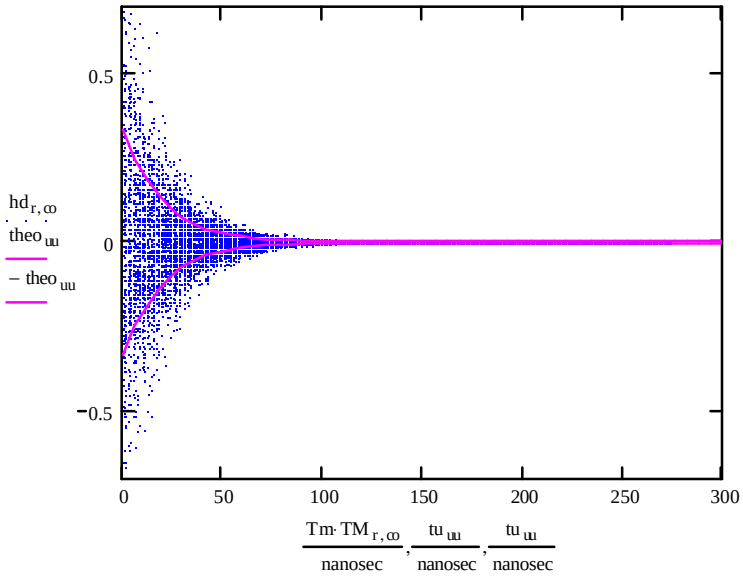

Figure 15. One Hundred realizations of the NLOS channel model at d=5 m.

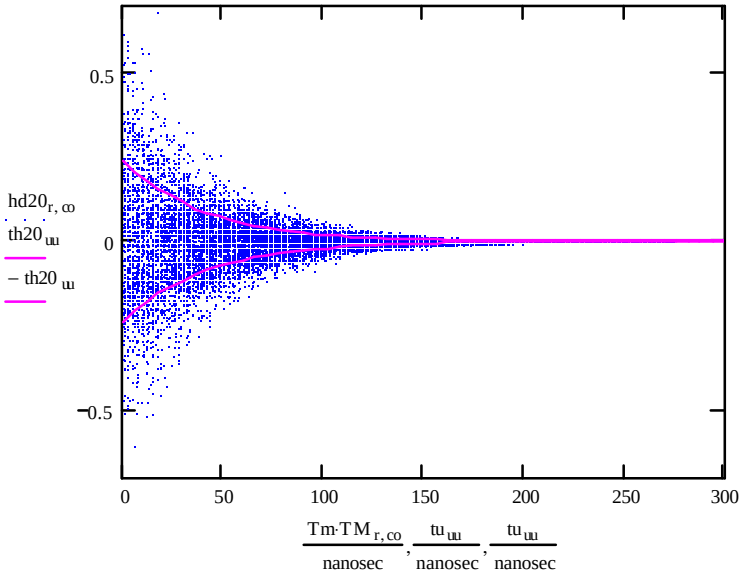

Figure 16. One Hundred realizations of the NLOS channel model at d=20 m.

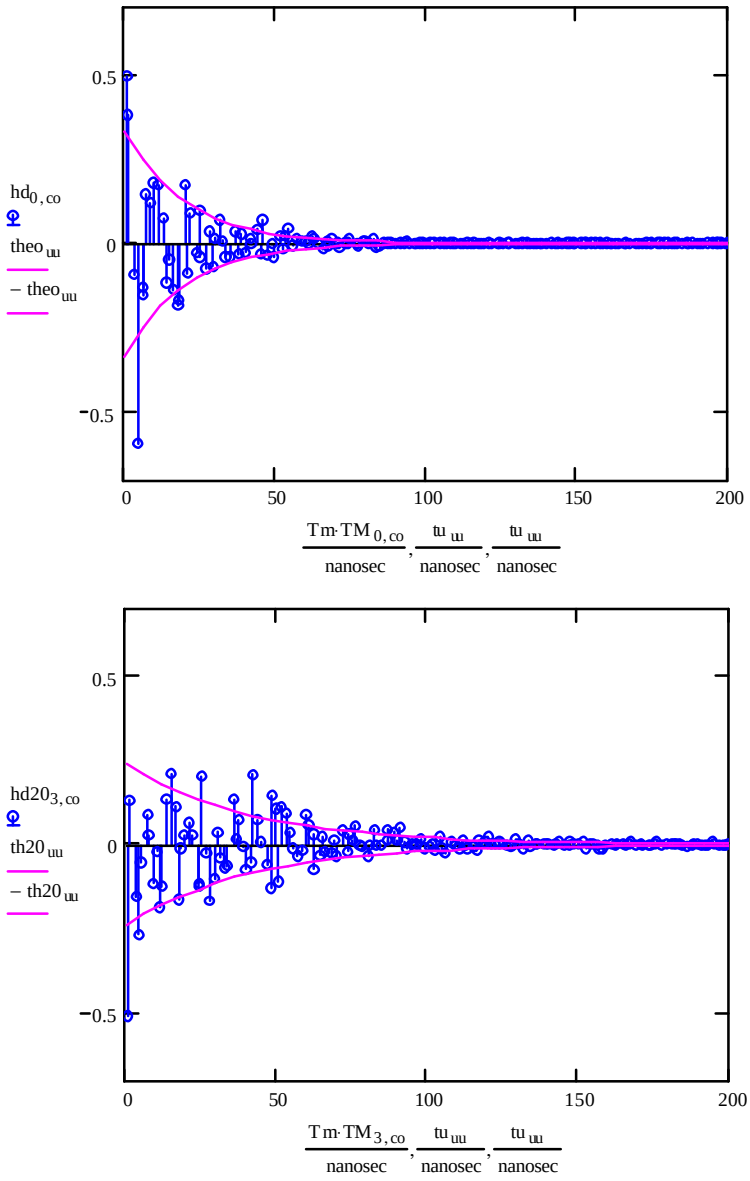

Figure 17. Two particlar realizations of the NLOS channel model at d=5 m (top), and d=20 m (bottom).

Notice in Figure 17 that amplitudes and the RMS delay spreads are a function of distance.

The recommended parameters are τ_0=4.5 ns, and D_t=1 m to approximately match the NLOS parameters of CM2, CM3, and CM4 in [IEEE802 02/249] at the required distances, see slide 34 of [IEEE802 04/504]. Specific recommended distance is 20 m. Direct path energy fraction K_F is a parameter that takes on values between 0 for a fully diffuse multipath and 1 for a pure line of sight free space path. K_F is related to the usual Ricean K-factor by $K_F=K/(1+K)$ or equivalently

$K=K_F/(1-K_F)$, where K_F is in the range [0, 1] and correspondingly K_F takes on the range [0, ∞]. Recommended values of K_F are 0, and a fully diffused multipath, 0.5 (half the reflected energy fraction in the LOS case. K_F=1 should be used to establish the radio performance in AWGN.

For both channel model components, the signal $S_N(t)$ contains all of the multipath components, weighted by the receiver antenna aperture, and by the receiver antenna efficiency. The method of signal detection, signal convolution the receiver filter, multiplication by the receiver template, and the signal processing will determine which and how many and how efficiently the multipath components are utilized.

the entire **case 2: N-LOS model** is specified by Equation (34), and supported by Equations (24), (25), (31), (32) and (33), as seen in the Appendix, along with the data files:

<15-04-0505-04-004a-NLOS_1000MHz_HK.txt>

<15-04-0505-04-004a-NLOS_1000MHz_TM.txt>

The data in the files is first scaled to the desired distance d by Equation (32). It is at this point that a distance specific RMS delay spread is associated with the multipath coefficients. The multipath components at this point are scaled in energy so that a natural propagation law includes spherical wave as well as dispersion into time.

$$hd_{r,co} := \left(\sqrt{1-\exp\left(\frac{-Tm}{\tau rmsN(d,Dt,\tau 0)}\right)}\right)\cdot hk_{r,co}\cdot\left(\exp\left(-\frac{Tm\cdot co}{2\cdot\tau 0}\right)\right)^{\frac{\tau 0}{\tau rmsN(d,Dt,\tau 0)}} \tag{32}$$

then,

$$H_{NLOS}(t)_r := Vfs(d)\cdot\sqrt{Kf}\cdot\delta(0) + \left(\sqrt{1-Kf}\right)\cdot\sum_{c=0}^{Kmax} hd_{r,c}\cdot\delta\left(t - Tm\cdot TM_{r,c}\right) \tag{33}$$

and the received signal is

$$S_N(t) := HN_{LOS}(t)\cdot\sqrt{Wrx} \tag{34}$$

The delay spread profile is defined by

$$\tau rmsN(d,Dt,\tau 0) := \tau 0\cdot\sqrt{\frac{d}{Dt}} \tag{31}$$

Recommended specific value for *d* is 20 and the corresponding RMS delay spread value is approximately 20 ns.

Body Proximity Effect and Antenna Efficiency:

The below 1000 MHz propagation model is intended for pulse and impulse doublets that contain low frequency energy and in particular energy below 200 MHz. Properly designed body proximate antennas at those frequencies can exhibit significant efficiency enhancements in the body resonant region for polarization coincident with the axis of the body. The measurements basis for the body enhancement problem are discussed in [Siwiak 1993], with the analysis and Mathcad templates available in [Siwiak 1995/8], and a further basis of measurements and analysis in [Durney 1986] and [DeLeon 1992]. The very low frequency approximation (below the human body resonance region) is based on very early work by Guy, finally reported in [Guy 1990].

Figure 18 shows the enhancement of antenna efficiency that results from placing a magnetic field antenna close to the human body. The ♦ symbols represent measurements correlated to an anthropometrically diverse group of human adults, while the solid line represents analytical results based on modeling the human body as a very simple "lossy wire" antenna, see [Guy 1990] and the implementation in [Siwiak 1995/8] and described in Figure 19. The dashed curve in Figure 18 represents analytical results based on a multilayer lossy cylinder analysis in [DeLeon 1992] and applied in [Siwiak 1995/8].

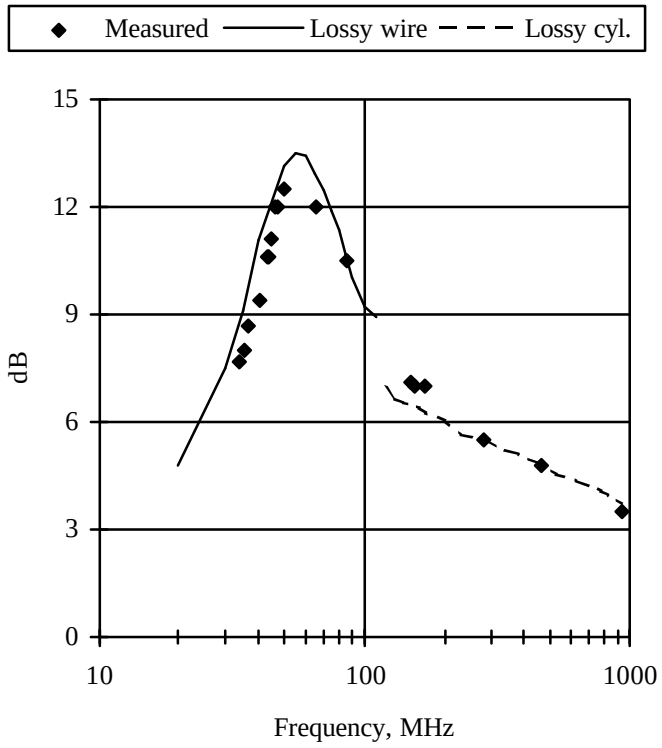

Figure 18. Magnetic field enhancement proximate to the human body. Source: [Siwiak 1995/9, used with permission].

The enhancement curve of Figure 18 would shift up in frequency for bodies that are significantly shorter in stature (children). This same "enhancement" mechanism is why RF exposure standards are much more severe in the 30 - 300 MHz frequency range.

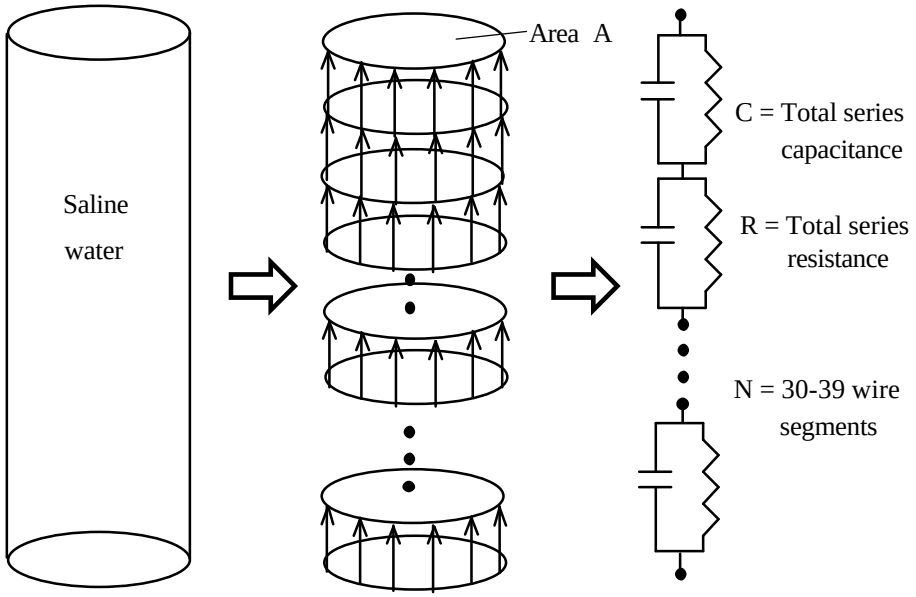

Figure 19. Analytical model for the human body in the body resonant region. Source: [Siwiak 1995/9, used with permission].

Thus the antenna efficiency term $\eta_{ant}(f)$ of Equation (25) will contain a body-proximate component based on Figure 18 for body worn devices. Time constraints preclude any further development of the topic here.

It is important to note that the azimuth pattern of a body proximate antennas varies with frequency. At low VHF frequencies the pattern is nearly omni-directional for the magnetic field. As frequency increases to the upper VHF range a shadow-related dip in the azimuth patter develops in the azimuth direction directly behind the body in the shadowed region. That dip becomes a deep null at UHF frequencies. The details and the analysis are in [Siwiak 1995/8].

Summary

A channel model has been developed and tailored for useat VHF and UHF. The special needs of ultra-wide band impulses and impulse doublets in this range are met by a line of sight model which deterministic imaging methodology to calculate a direct component and 13 strongest multipath reflections within a room. Only the wall reflections are considered, in so far as the wavelengths under consideration approach several meters. This LOS model brings into play a severe multipath distortion phenomenon based on the strict correlation imposed by the wall boundary conditions between the multipath components. In other words, in LOS case, the

multipath is not stochastic. The total energy transferred between antennas in the room is more than from the direct path alone even though the actual propagation by spherical waves (square law). This effect has often been "curve fit" in other models by unrealistic propagation coefficients smaller than 2. The RMS delay spread of the multipath was seen to be a linear function of the room dimensions.

A non-line of sight case of the VHF-UHF channel model uses a stochastic method to generate exponentially weighted multipath components for which the delay spread increases with distance, as is seen in measurement of both UWB impulses and of narrow band signals. The model generates multipath *at any distance and with RMS delay spread varying with distance* from a common set of randomly generated trials by using a simple scaling formula developed here, which includes the functional form of the RMS delay versus distance. The increase of RMS delay spread with distance is one of the reasons why the apparent power law of propagation appears higher than 2. Energy is spread spherically, but energy is additionally 'robbed' and dispersed in time (increasing multipath with distance). The model correctly accounts for this effect, and thus realistically models energy per component versus distance. Additionally, the total energy in the NLOS case is divided between a direct path and diffuse multipath energy to realistically model signals with Ricean statistics.

Finally, the antenna efficiency and antenna pattern distortion due to the body-proximate effect are captured in an antenna efficiency term in the model. It is pointed out, and referenced extensively, that a properly designed antenna close to the human body looks like a lossy wire antenna having the body longitudinal dimensions. The effect enhances link margin in the VHF and lower UWF frequencies, but begins to exhibit a deep pattern null at the upper VHF and the UHF frequencies.

References

[Cassiolli 2002] D. Cassioli, Moe Z. Win and Andreas F. Molisch, "The Ultra-Wide Bandwidth Indoor Channel: from Statistical Model to Simulations", IEEE Journal on Selected Areas on Communications, Vol. 20, pp. 1247-1257, August 2002.

[Canada 2004] Canada, INFO DOCUMENT, "Characterization of ultra-wideband (UWB) pulse distortion in time domain," ITU Document 1-8/203-E, 27 October 2004.

[DaSilva 2003] Da Silva, C.R.C.M. Milstein, L.B., "Spectral-encoded UWB communication systems," 2003 IEEE Conference on Ultra Wideband Systems and Technologies, 16-19 Nov. 2003, pp. 96- 100.

[DeLeon 1992] L. Ponce de Leon, "Modeling and measurement of the response of small antennas near multilayered two or three dimensional dielectric bodies," Ph.D. Dissertation, Florida Atlantic University, 1992.

[Durney 1986] C. H. Durney, H. Massoudi, M. F. Iskander, Radiofrequency Radiation Dosimetry Handbook, Fourth Edition, USAFSAM-TR-85-73, USAF School of Aerospace, Brooks AFB, TX 78235, October 1986.

[Guy 1990] A. W. Guy, "Analysis of EMP induced currents in human body by NEC Method of Moments," Proc. of the Twelfth Annual International Conference of the IEEE Engineering in Medicine and Biology Society, Philadelphia, PA, Nov. 1-4, 1990, pp. 1547-1548.

[Honch 1992] W. Honcherenko, H. L. Bertoni, "Mechanisms governing UHF propagation on single floors in modern office buildings," IEEE Transactions on Vehicular Technology, Vol. 41, No. 4, November 1992, pp. 496-504.

[IEEE802 02/249] "Channel Modeling Sub-committee Report – Final," IEEE P802.15 Working Group for Wireless Personal Area Networks (WPANs), IEEE document P802.15-02/249r0-SG3a, Dec, 2002. (Online): http://grouper.ieee.org/groups/802/15/pub/2002/Nov02/

[IEEE802 02/282] "UWB Indoor Model," IEEE P802.15 Working Group for Wireless Personal Area Networks (WPANs), IEEE document P802.15-02/282r1-SG3a, July 8, 2002. (Online): http://grouper.ieee.org/groups/802/15/pub/2002/Jul02/

[IEEE802 04/504] IEEE P802.15 Working Group for Wireless Personal Area Networks (WPANs), IEEE document P802.15-04/504r1-TG3a, Sept, 2004, 15-04-0504-01-003a-ds-uwb-no-response-eq-sop.ppt

[Jakes 1974] W. C. Jakes. Microwave Mobile Communications, American Telephone and Telegraph Co., 1974, reprinted: IEEE Press, Piscataway, NJ, 1993.

[Siwiak 1993] K. Siwiak, L. Ponce de Leon and W. M. Elliott III, "Pager sensitivities, open field antenna ranges, and simulated body test devices: analysis and measurements," First Annual RF / Microwave Non-Linear Simulation Technical Exchange, Motorola, Inc., Plantation, FL, 26 March 1993.

[Siwiak 1995/8] K. Siwiak, **Radiowave Propagation and Antennas for Personal Communications**, Boston MA: Artech House 1995 (second ed: 1998).

[Siwiak 2003] K. Siwiak, H. L. Bertoni, and S. Yano, "On the relation between multipath and wave propagation attenuation," Electronic Letters, 9th January 2003, Volume 39 Number 1, pp. 142-143.

[Siwiak 2004] K. Siwiak and D. McKeown, **Ultra-wide Band Radio Technology**, Chichester, England: Wiley and Sons, 2004.

[Yano 2002] S. M. Yano: "*Investigating the ultra-wideband indoor wireless channel,*" Proc. IEEE VTC2002 Spring Conf., May 7-9, 2002, Birmingham, AL, Vol. 3, pp. 1200-1204.

APPENDIX

Mathcad code for the VHF-UHF Channel model Components

Although the Mathcad code contains a rich set of illustrative examples, details and check cases, the entire **case 1: LOS model** is specified by Equation (26), and supported by Equations (23a), (24),and (25) are needed along with the data file:

<15-04-0505-04-004a-los_1000MHz.txt>

Likewise, the entire **case 2: N-LOS model** is specified by Equation (34), and supported by Equations (24), (25), (31), (32) and (33) along with the data files:

<15-04-0505-04-004a-NLOS_1000MHz_HK.txt>

<15-04-0505-04-004a-NLOS_1000MHz_TM.txt>

UWB Channel Model Components for use below 1 GHz
- Kai Siwiak

Preliminary Draft: 10 Sep 2004; rev0 12 Oct 2004; rev1 18 Oct 2004; rev2 27 Oct 2004
rev3 01 Nov 2004; final version rev4 07 Nov 2004

The 100 MHz channel model comprises two components. The first is a LOS in-room component that captures the major reflection sources at low frequencies, which are the walls and floor for the LOS case. The second is a N-LOS component which is based on the Jakes [Jakes 1974] model with exponential energy density profile (EDP). The multipath UWB pulses and impulses are exponentially distributed, their arrival interval is randomly distributed in windows of duration Ts.

For both cases a signal S(t) contains all of the multipath components, weighted by the receiver antenna aperture, and by the receiver antenna efficiency. The method of signal detection, signal convolution the receiver filter, multiplication by the receiver template, and the signal processing will determine which and how many and how efficiently the multipath components are utilized.

Case 1 - The LOS Model

LOS: attenuation is free space intergal over PSD: $d<(RoomX^2+RoomY^2)^{1/2}$ m

- Direct plus with Γ^{-2} power additional single reflection multipaths; Γ^4 from corner reflections
- Multipath is derived from 13 primary reflections of a room model:
  - 4 principal reflections from the walls
  - 1 ground reflection
  - 4 principal corner reflections
  - 4 secondary wall reflections
- Multiple realizations are utilized.

The following parameters specific the UWB radio performance in a room-LOS condition:
(1) Room dimensions RoomX and RoomY, and minimum distance to a wall dt, wall thickness wth
(2) Antenna height ranges between Hlow and Hhigh
(2) Radiated power spectral density EIRPsd(f)
(3) Receiver antenna aperture Ae
(4) Multipath signal profile S(t)
(5) Average reflection coefficient Γm

Derived parameters include:
- RMS delay spread τrms,
- the mean ray arrival rate Ts
- excess energy factor in the room is Wx

Total energy is accounted for in the room. The "excess" energy in the room should be balanced by the average wall-transmitted energy.

The geometry for the LOS in-room model is shown in Figure 1a.

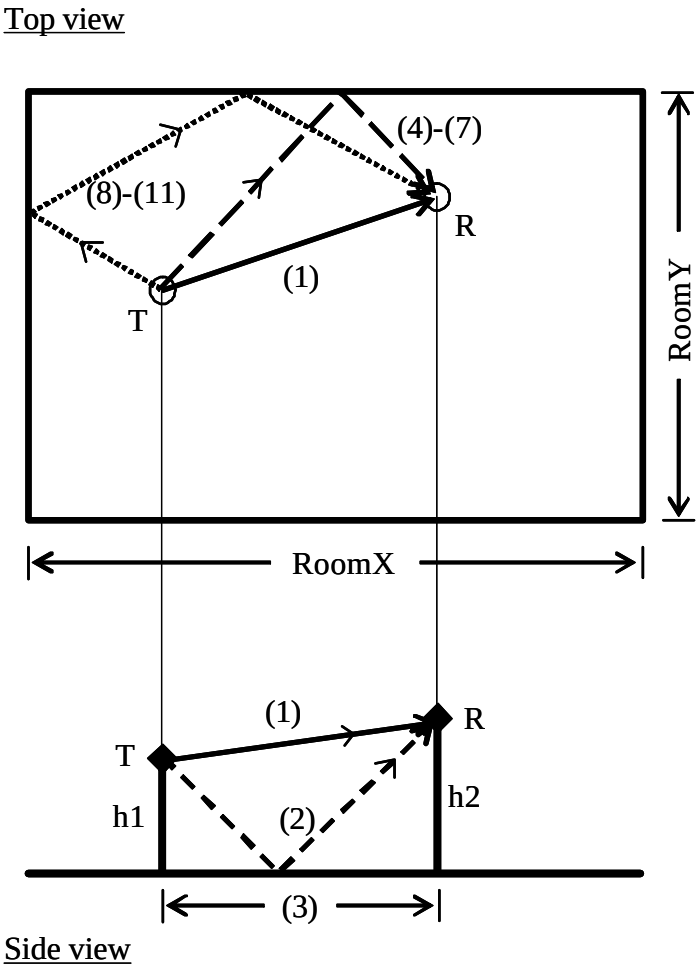

Figure 1a. Top and side views of signal paths inside a room.

Reflections are shown for only one wall and for one corner. All four wall and corners are considered in the model.

The secondary reflections from energy bouncing between walls is shown in Figure 1b.

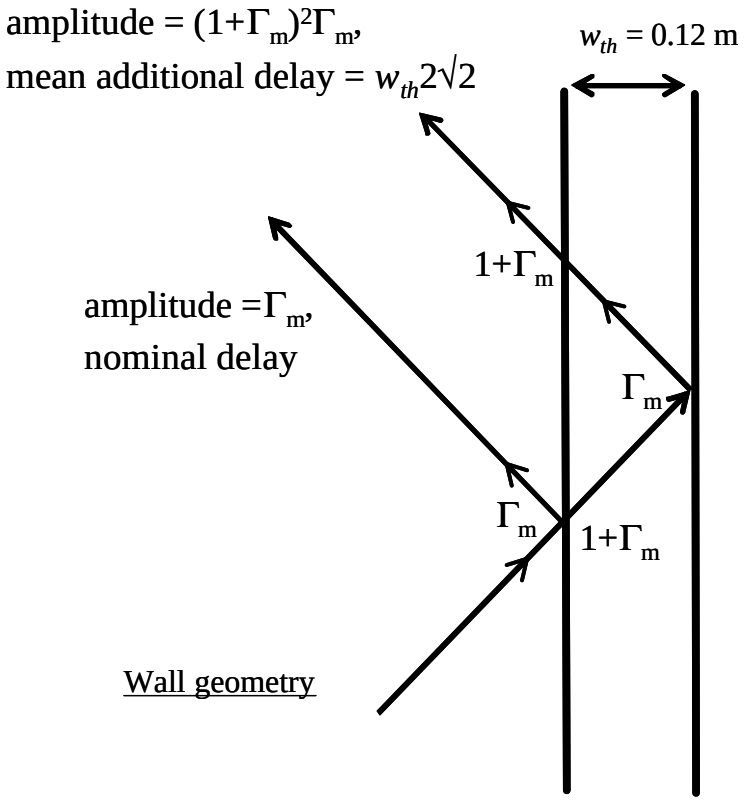

Figure 1b. Secondary reflection from the wall are attenuated about 20 dB.

Case 2 - Non-Line of Sight Multipath Model

The Jakes [Jakes 1974] model with exponential EDP will be applied, here for UWB pulses in non-line of sight (NLOS) cases. Thus the multipath impulses are exponentially distributed, their arrival interval is randomly distributed in windows of duration Ts. The delay spread parameter is a function of distance, [Siwiak 2003], and here is modeled by the square root of distance, see slide 34 of [IEEE802 04/504]. This naturally results in a 2.5 power law in propagation as a function of distance.

The following parameters specific the UWB radio performance in a N-LOS condition:
(1) RMS delay spread parameter $\tau 0$ s and distance Dt
(2) Mean interval between rays Tm s
(3) Fraction of energy in direct ray Kf
(4) Radiated power spectral density EIRPsd(f)
(5) Receiver antenna aperture Ae
(6) Multipath signal profile SN(t)

For both channel model components, the signal SN(t) contains all of the multipath components, weighted by the receiver antenna aperture, and by the receiver antenna efficiency. The method of signal detection, signal convolution the receiver filter, multiplication by the receiver template, and the signal processing will determine which and how many and how efficiently the multipath components are utilized.

References:

[Honch 1992] W. Honcherenko, H. L. Bertoni, "Mechanisms governing UHF propagation on single floors in modern office buildings," IEEE Transactions on Vehicular Technology, Vol. 41, No. 4, November 1992, pp. 496-504.

[Jakes 1974] W. C. Jakes. Microwave Mobile Communications, American Telephone and Telegraph Co., 1974, reprinted: IEEE Press, Piscataway, NJ, 1993.

[Cassiolli 2002] D. Cassioli, Moe Z. Win and Andreas F. Molisch, “The Ultra-Wide Bandwidth Indoor Channel: from Statistical Model to Simulations”, IEEE Journal on Selected Areas on Commun., Vol. 20, pp. 1247-1257, August 2002.

[Siwiak 2003] K. Siwiak, H. Bertoni, and S. Yano, “On the relation between multipath and wave propagation attenuation,” Electronic Letters, 9th January 2003, Volume 39 Number 1, pp. 142-143.

[IEEE802 02/249] “Channel Modeling Sub-committee Report – Final,” IEEE P802.15 Working Group for Wireless Personal Area Networks (WPANs), IEEE document P802.15-02/249r0-SG3a, Dec, 2002. (Online): http://grouper.ieee.org/groups/802/15/pub/2002/Nov02/

[IEEE802 04/504] IEEE P802.15 Working Group for Wireless Personal Area Networks (WPANs), IEEE document P802.15-04/504r1-TG3a, Sept, 2004, 15-04-0504-01-003a-ds-uwb-no-response-eq-sop.ppt

Case 1: Line of Sight Multipath Model

Constants: speed of propagation, m/s	$c := 299792458$	$\mu := 4\cdot\pi\cdot 10^{-7}$
	$MHz := 10^{6}$	$nanosec := 10^{-9}$
Room dimensions for LOS case, m	$RoomX := 3.7$	$RoomY := 4.6$
Minimum distance from walls, and the wall thickness, m	$dt := 0.1$	$wth := 0.12$
Antenna heights between above the floor, m	$h1 := 1.0$	$h2 := 2$

A room in an office or industrial area is modeled as 4 walls with dimensions RoomX and RoomY (m). The radio devices are between heights h1 and h2, and are at least distance dt from any wall. The reflection coefficient Γ is a single average value derived from [Honch 1992].

A direct path and ground reflected path between two radios in the same room is first selected randomly. Then the four principle wall reflections are considered.

The direct and ground reflected path are found from:

$$d(x1,x2,y1,y2,h1,h2) := \sqrt{(x2-x1)^2+(y2-y1)^2+(h2-h1)^2} \quad (1)$$

$$gnd(x1,x2,y1,y2,h1,h2) := \sqrt{(x2-x1)^2+(y2-y1)^2+(h2+h1)^2} \quad (2)$$

Separation distance projected on the ground is

$$dg(x1,x2,y1,y2) := \sqrt{(x2-x1)^2+(y2-y1)^2} \quad (3)$$

The principal reflected paths are the specular images of the direct path.

$$r1(x1,x2,y1,y2,h1,h2) := \sqrt{(x2-x1)^2+(y2+y1)^2+(h2-h1)^2} \quad (4)$$

$$r2(x1,x2,y1,y2,h1,h2) := \sqrt{(x2-x1)^2+(2\cdot RoomY-y2-y1)^2+(h2-h1)^2} \quad (5)$$

$$r3(x1,x2,y1,y2,h1,h2) := \sqrt{(x2+x1)^2+(y2-y1)^2+(h2-h1)^2} \quad (6)$$

$$r4(x1,x2,y1,y2,h1,h2) := \sqrt{(2\cdot RoomX-x2-x1)^2+(y2-y1)^2+(h2-h1)^2} \quad (7)$$

Corner bank reflection paths - two wall reflections - there are two possibilities for projecting each corner image, but both result in the same path distance:

$$c1(x1,x2,y1,y2,h1,h2) := \sqrt{(x2+x1)^2+(y2+y1)^2+(h2-h1)^2} \quad (8)$$

$$c2(x1,x2,y1,y2,h1,h2) := \sqrt{(x2+x1-2\cdot RoomX)^2+(y2+y1)^2+(h2-h1)^2} \quad (9)$$

$$c3(x1,x2,y1,y2,h1,h2) := \sqrt{(x2+x1-2\cdot RoomX)^2+(y2+y1-2\cdot RoomY)^2+(h2-h1)^2} \quad (10)$$

$$c4(x1,x2,y1,y2,h1,h2) := \sqrt{(x2+x1)^2+(y2+y1-2\cdot RoomY)^2+(h2-h1)^2} \quad (11)$$

Equations (1)-(11) are exercised to compute a statistically significant number of randomly selected paths in the room, and the specular reflected paths are also computed. Nrnd is the counter limit for index i and is set to several thousands to get statistically valid results. Coordinates ($XR1_i$, $YR1_i$, $H1_i$) and ($XR2_i$, $YR2_i$,$H2_i$) of the two direct path endpoints are selected.

Number of trials is: $Nrnd := 39999$ $i := 0..Nrnd$ $dH := h2 - h1$

$$X1r_i := rnd(RoomX - 2\cdot dt) + dt \quad Y1r_i := rnd(RoomY - 2\cdot dt) + dt \quad H1_i := h1 + rnd(dH)$$
$$X2r_i := rnd(RoomX - 2\cdot dt) + dt \quad Y2r_i := rnd(RoomY - 2\cdot dt) + dt \quad H2_i := h1 + rnd(dH) \tag{12}$$

Then the direct D_i distances and ground reflected Gr distances are computed, and the principle specular wall reflection distances $R1_i$, $R2_i$, $R3_i$, $R4_i$ are computed. Corner reflection C1, C2, C3, C4 are found. The path lengths in excess of the direct path are $eR1_i$, $eR2_i$, $eR3_i$, and $eR4_i$; and eC1, eC2, eC3, eC4.

$$D_i := d(X1r_i, X2r_i, Y1r_i, Y2r_i, H1_i, H2_i) \qquad Dg_i := dg(X1r_i, X2r_i, Y1r_i, Y2r_i)$$
$$R1_i := r1(X1r_i, X2r_i, Y1r_i, Y2r_i, H1_i, H2_i) \qquad eR1_i := R1_i - D_i$$
$$R2_i := r2(X1r_i, X2r_i, Y1r_i, Y2r_i, H1_i, H2_i) \qquad eR2_i := R2_i - D_i$$
$$R3_i := r3(X1r_i, X2r_i, Y1r_i, Y2r_i, H1_i, H2_i) \qquad eR3_i := R3_i - D_i$$
$$R4_i := r4(X1r_i, X2r_i, Y1r_i, Y2r_i, H1_i, H2_i) \qquad eR4_i := R4_i - D_i$$
$$Gr_i := gnd(X1r_i, X2r_i, Y1r_i, Y2r_i, H1_i, H2_i) \qquad eG_i := Gr_i - D_i \tag{13}$$
$$C1_i := c1(X1r_i, X2r_i, Y1r_i, Y2r_i, H1_i, H2_i) \qquad eC1_i := C1_i - D_i$$
$$C2_i := c2(X1r_i, X2r_i, Y1r_i, Y2r_i, H1_i, H2_i) \qquad eC2_i := C2_i - D_i$$
$$C3_i := c3(X1r_i, X2r_i, Y1r_i, Y2r_i, H1_i, H2_i) \qquad eC3_i := C3_i - D_i$$
$$C4_i := c4(X1r_i, X2r_i, Y1r_i, Y2r_i, H1_i, H2_i) \qquad eC4_i := C4_i - D_i$$

Additional mean delay due to the first order internal wall reflection is:

$$eW := 2\cdot\sqrt{2}\cdot wth \qquad eW = 0.339 \quad m \tag{13a}$$

View a subset of the first 100 points: $xs := 99$ $x := 0..xs$

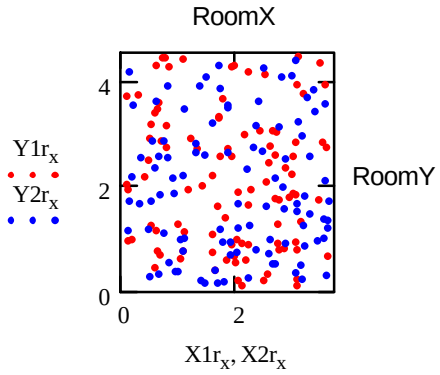

Figure 2. A sampling of the total points (X1, Y1) and (X2, Y2).

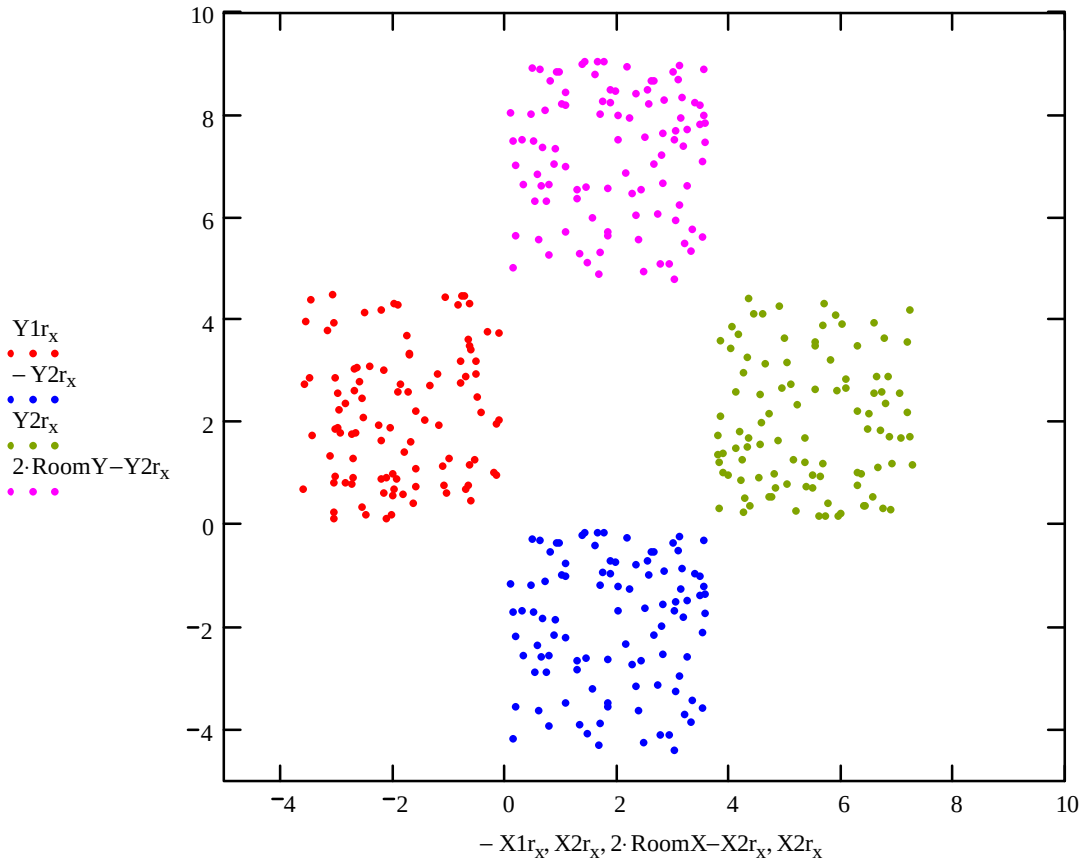

Figure 3. Images in the room walls of the reflection points. C1 are lower left and C2 are lower right, C3 are upper right and C4 are upper left.

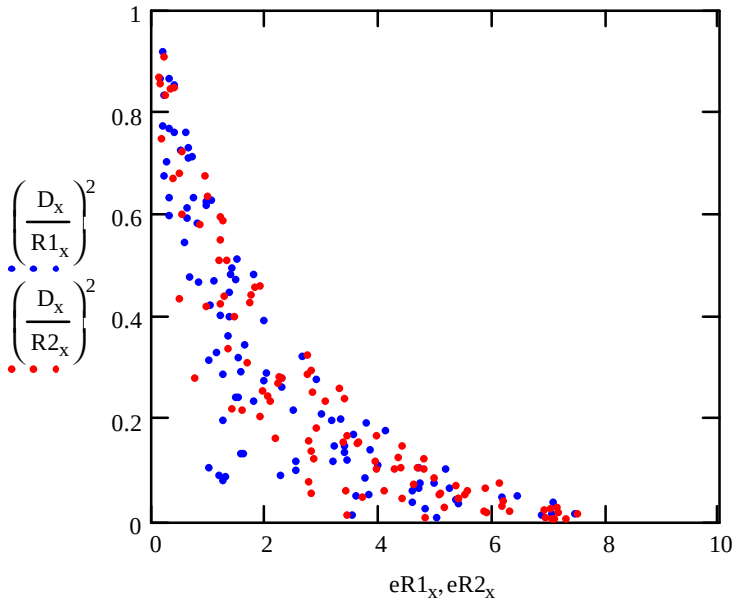

Figure 4. Energy delay profile (EDP) vs. excess delay: R1, R2,m. The excess delays is associated with the Y dimension of the room.

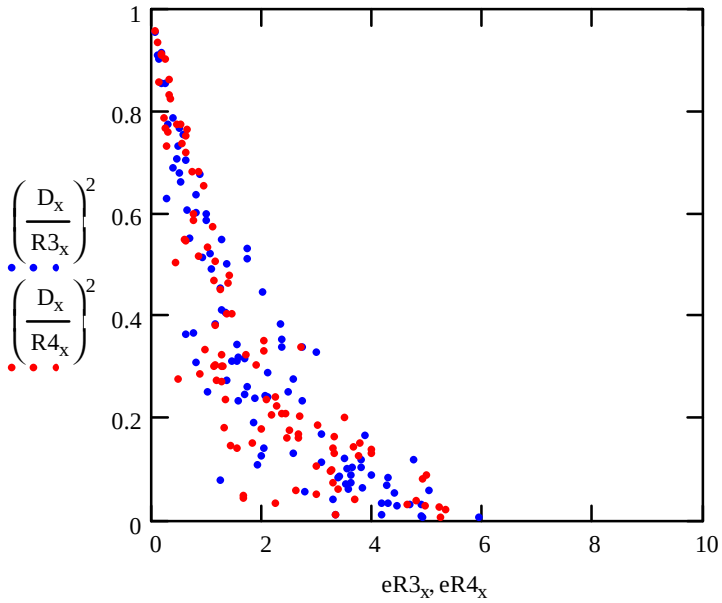

Figure 5. Energy delay profile vs. excess delay, R3, R4, m. The excess delays are associated with the X dimension of the room.

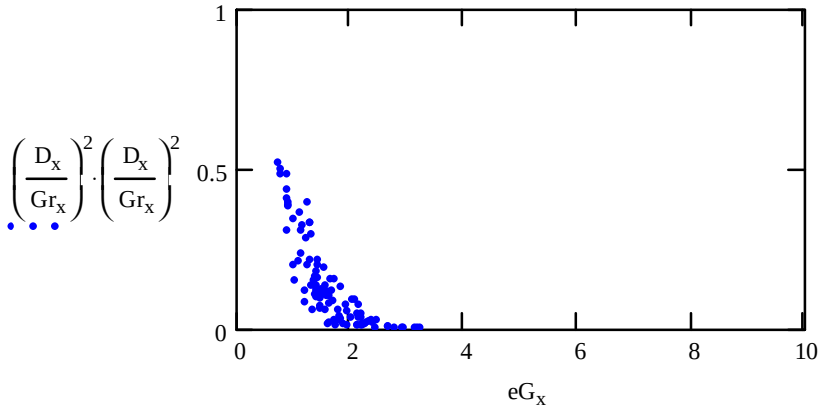

Figure 6. Energy delay profile vs. excess delay, m, for the ground reflection Gr.

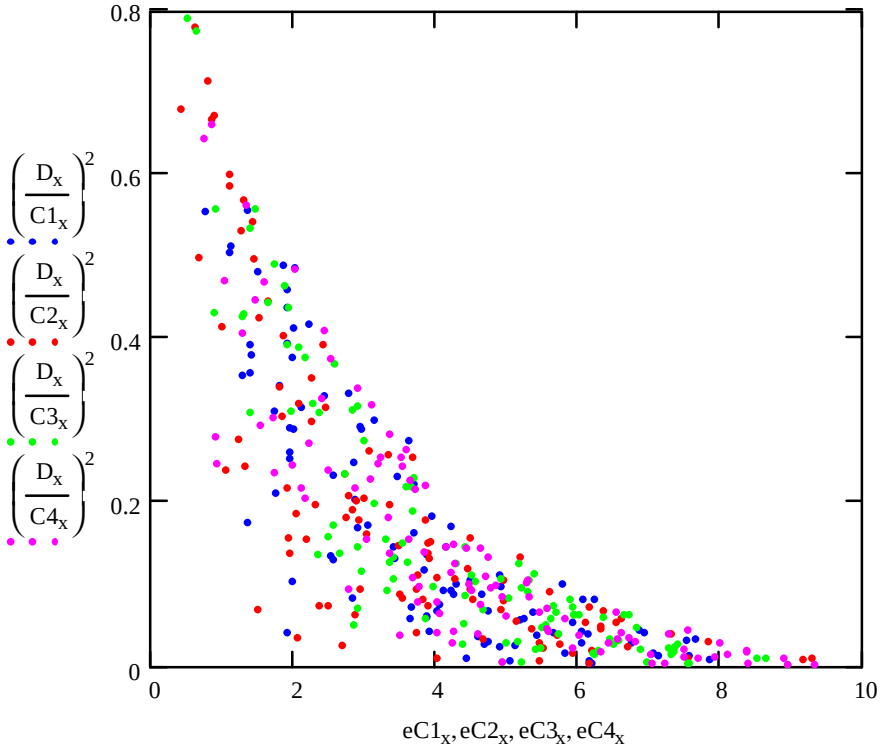

Figure 7. Energy delay profile vs. excess delay in m, for the corner reflections.

Reflections from the floor and walls.

Reflection coefficient from concrete or plasterboard is between 0.3 for 0 deg, 1 for grazing angle of incidence, see [Honch 1992].

$j := 0..9$

$\Gamma_j :=$

0.3
0.3
0.3
0.3
$0.3 + \frac{0.7}{5}$
$0.3 + 2\cdot\frac{.7}{5}$
$0.3 + 3\cdot\frac{.7}{5}$
$0.3 + 4\cdot\frac{.7}{5}$
1
1

$\Gamma_j =$

0.3
0.3
0.3
0.3
0.44
0.58
0.72
0.86
1
1

$j =$

0
1
2
3
4
5
6
7
8
9

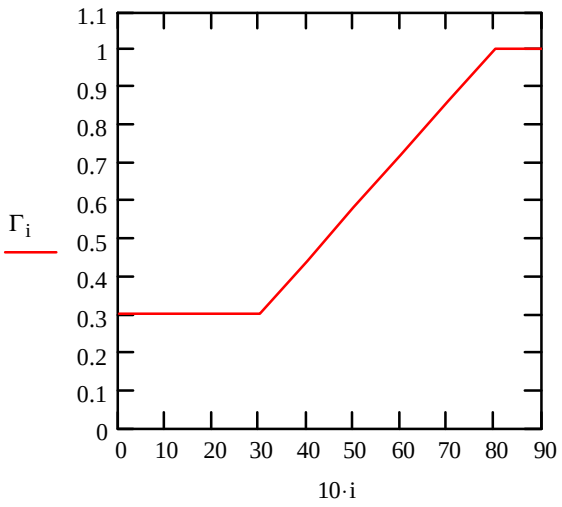

Figure 8. Reflection coefficient vs. incident angle for concrete and plaster board walls. [Honch 1992].

$\Gamma m := -mean(\Gamma)$ $\Gamma m = -0.58$ (14)

$20\cdot\log(|\Gamma m|) = -4.731$

Considering transmissions through walls:

Normal incidence transmission $20\cdot\log(1 - .3) = -3.098$

Average incidence transmission $Tm := 1 + \Gamma m$ $20\cdot\log(Tm) = -7.535$

Secondary reflections involve a transmission through one wall interface followed by a reflection from the back side of the wall followed by the tranmission through the front side of the wall. The secondary reflection are thus on the average down by:

$$\Gamma_{2m} := -\frac{1}{9}\cdot\sum_{j=1}^{9}\left[(1-\Gamma_j)^2\cdot\Gamma_j + .001\right] \quad (15)$$

$\Gamma_{2m} = -0.085$ $20\cdot\log(|\Gamma_{2m}|) = -21.428$ dB

The average secondary reflection is about 20 dB attenuated and will be included.

Higher order wall internal reflections are omitted; the next component is ~35 dB below the direct:

$$\Gamma_{3m} := -\frac{1}{9}\cdot\sum_{j=1}^{9}\left[(1-\Gamma_j)^2\cdot(\Gamma_j)^3 + .001\right] \qquad 20\cdot\log(|\Gamma_{3m}|) = -35.474 \quad \text{dB}$$

Second order corner reflections will be omitted, they are more than 20 dB down:

$$\Gamma_{2cm} := -\frac{1}{9}\cdot\sum_{j=1}^{9}\left[(1-\Gamma_j)^2\cdot(\Gamma_j)^2 + .001\right] \qquad 20\cdot\log(|\Gamma_{2cm}|) = -29.078 \quad \text{dB}$$

One secondary wall reflection is included. Its amplitude is about 20 dB below the direct component.

The additional delay of the secondary reflection is:

$eW = 0.339$ m

The included reflection components inside the room are:

- 4 principal reflections from the walls (of order Γ_m = -5 dB)
- 1 ground reflection (of order $\cos(\theta)\Gamma_m$ = -7 dB)
- 4 principal corner reflections (of order Γ_m^2 = -10 dB)
- 4 secondary reflections from the walls (of order $(1+\Gamma_m)^2\Gamma_m$ = -21 dB)

Three distinct groupings of the EDP (energy delay profile) are evident in Figures 4-7. These occur because there are three distinct mechanisms in operation. the room is a rectangle so reflections associated with the width and length will cluster differently. Also the ground reflection depends only on separation distance and on antenna heights h1 and h2.

The rms delay spread τrms is the second central moment of the power delay profile for each of path. The energies relative to a direct path are the square of the distance ratio: $(D/R)^2$. The ground reflected component is out of the plane of the other components, and its energy is additionally weighted by the the projection of the vertical field vector on the receive antenna, via the ground reflection hence the ground component relative energy is approximately $(1/Gr)^2(D/Gr)4$. The delay spread is found from

$$\begin{aligned} dm_i := & \left[\left(\frac{D_i}{R1_i}\right)^2 \cdot eR1_i + \left(\frac{D_i}{R2_i}\right)^2 \cdot eR2_i + \left(\frac{D_i}{R3_i}\right)^2 \cdot eR3_i + \left(\frac{D_i}{R4_i}\right)^2 \cdot eR4_i + \left(\frac{Dg_i}{Gr_i}\right)^2 \cdot \left(\frac{D_i}{Gr_i}\right)^4 \cdot eG_i\right] \cdot \Gamma m^2 \ ... \\ & + \left[\begin{array}{l} \left(\frac{D_i}{R1_i}\right)^2 \cdot \left(eR1_i + eW\right) + \left(\frac{D_i}{R2_i}\right)^2 \cdot \left(eR2_i + eW\right) \ ... \\ + \left(\frac{D_i}{R3_i}\right)^2 \cdot \left(eR3_i + eW\right) + \left(\frac{D_i}{R4_i}\right)^2 \cdot \left(eR4_i + eW\right) \end{array}\right] \cdot \Gamma_{2m}{}^2 \ ... \\ & + \left[\left(\frac{D_i}{C1_i}\right)^2 \cdot eC1_i + \left(\frac{D_i}{C2_i}\right)^2 \cdot eC2_i + \left(\frac{D_i}{C3_i}\right)^2 \cdot eC3_i + \left(\frac{D_i}{C4_i}\right)^2 \cdot eC4_i\right] \cdot \Gamma m^4 \end{aligned} \tag{16}$$

$$\begin{aligned} dm2_i := & \left[\begin{array}{l} \left(\frac{D_i}{R1_i}\right)^2 \cdot \left(eR1_i\right)^2 + \left(\frac{D_i}{R2_i}\right)^2 \cdot \left(eR2_i\right)^2 + \left(\frac{D_i}{R3_i}\right)^2 \cdot \left(eR3_i\right)^2 \ ... \\ + \left(\frac{D_i}{R4_i}\right)^2 \cdot \left(eR4_i\right)^2 + \left(\frac{Dg_i}{Gr_i}\right)^2 \cdot \left(\frac{D_i}{Gr_i}\right)^4 \cdot \left(eG_i\right)^2 \end{array}\right] \cdot \Gamma m^2 \ ... \\ & + \left[\begin{array}{l} \left(\frac{D_i}{R1_i}\right)^2 \cdot \left(eR1_i + eW\right)^2 + \left(\frac{D_i}{R2_i}\right)^2 \cdot \left(eR2_i + eW\right)^2 \ ... \\ + \left(\frac{D_i}{R3_i}\right)^2 \cdot \left(eR3_i + eW\right)^2 + \left(\frac{D_i}{R4_i}\right)^2 \cdot \left(eR4_i + eW\right)^2 \end{array}\right] \cdot \Gamma_{2m}{}^2 \ ... \\ & + \left[\left(\frac{D_i}{C1_i}\right)^2 \cdot \left(eC1_i\right)^2 + \left(\frac{D_i}{C2_i}\right)^2 \cdot \left(eC2_i\right)^2 + \left(\frac{D_i}{C3_i}\right)^2 \cdot \left(eC3_i\right)^2 + \left(\frac{D_i}{C4_i}\right)^2 \cdot \left(eC4_i\right)^2\right] \cdot \Gamma m^4 \end{aligned} \tag{17}$$

$$W_i := \left[\left(\frac{D_i}{R1_i}\right)^2 + \left(\frac{D_i}{R2_i}\right)^2 + \left(\frac{D_i}{R3_i}\right)^2 + \left(\frac{D_i}{R4_i}\right)^2\right]\cdot\left(\Gamma m^2 + \Gamma_{2m}{}^2\right) + \left(\frac{Dg_i}{Gr_i}\right)^2\cdot\left(\frac{D_i}{Gr_i}\right)^4\cdot\Gamma m^2 \ldots$$
$$+\left[\left(\frac{D_i}{C1_i}\right)^2 + \left(\frac{D_i}{C2_i}\right)^2 + \left(\frac{D_i}{C3_i}\right)^2 + \left(\frac{D_i}{C4_i}\right)^2\right]\cdot\Gamma m^4 \qquad (18)$$

The "total" energy in the room is Wx times the direct path energy: $Wx := mean(W) + 1$ $10\cdot\log(Wx) = 1.897$ dB

$10\cdot\log(Wx - 1) = -2.614$ dB

$$d2rms_i := \sqrt{\frac{dm2_i}{W_i} - \left(\frac{dm_i}{W_i}\right)^2} \qquad drms := mean(d2rms) \qquad (19)$$

$max(d2rms) = 1.72$ $min(d2rms) = 0.188$ $drms = 1.197$ meters

Finally the rms delay spread τrms is found

$$\tau rms := \frac{drms}{c} \qquad (20)$$

and its value for the selected case is

$\tau rms\cdot 10^9 = 3.991$ nS $\frac{max(d2rms)}{c}\cdot 10^9 = 5.736$ nS

The mean ground refelcted component is

$$Ground_i := \left(\frac{D_i}{Gr_i}\right)^4\cdot eG_i \qquad GdB := mean(Ground) \qquad 10\cdot\log(GdB) = -7.561$$

The mean, max and min ranges are: $mean(D) = 2.12$ $max(D) = 5.233$ $min(D) = 0.041$

The maximum possible LOS range is: $Rmax := \sqrt{(RoomX - 2\cdot dt)^2 + (RoomY - 2\cdot dt)^2 + dH^2}$

$Rmax = 5.711$ m

Max possible corner to corner distance is: $Rmax := \sqrt{(RoomX)^2 + (RoomY)^2 + dH^2}$

$Rmax = 5.987$ m

Figure 9 shows the EDPs vs. excess delays for all three sets of of reflections. The secondary wall reflections are not shown in this figure. Note the ground reflections (magenta) follow a narrow range of possibilities. An exponential EDP with delay spread τrms is shown as the black trace, but it does not model the room reflections very well. Since the room primary reflections are entirely deterministic, these will be used as the model. The clear areas hugging the abscissa and the ordinate result from setting the two antenna heights to different values.

$UU := 50$ $\quad scale := 0.2$

$uu := 0..UU$ $\quad p := 2$ $\quad f_{uu} := \exp\left(\frac{-uu \cdot scale}{drms \cdot 2}\right)$

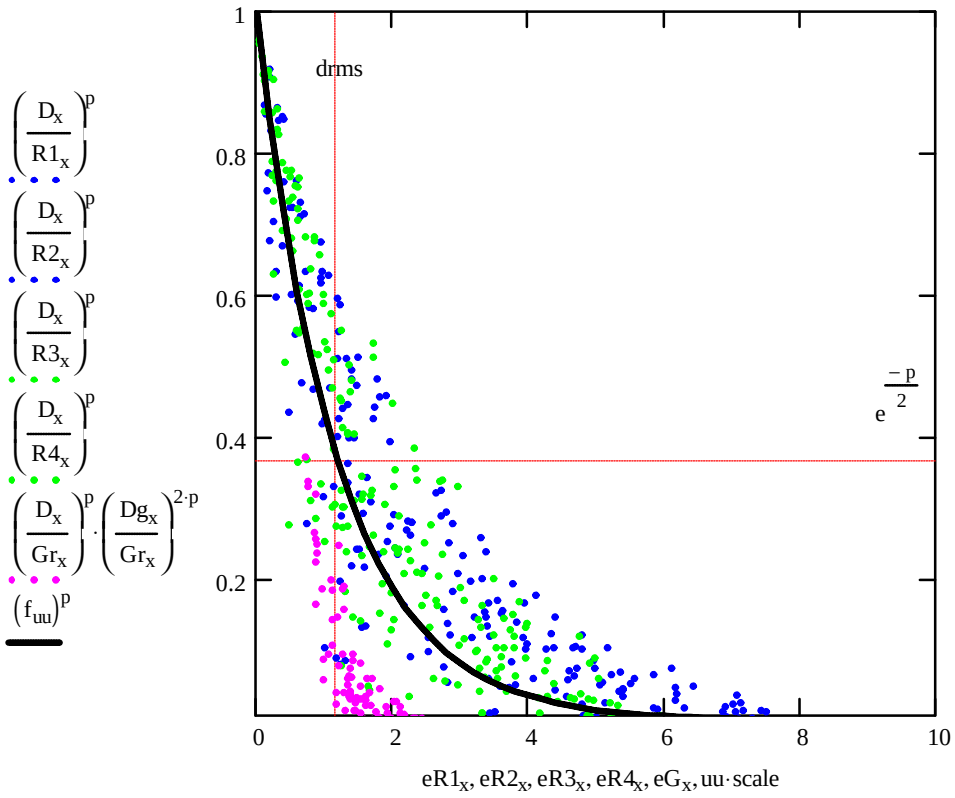

Figure 9. Energy delay profile vs. excess delay in m for primary wall-reflected components compared with exponential EDP.

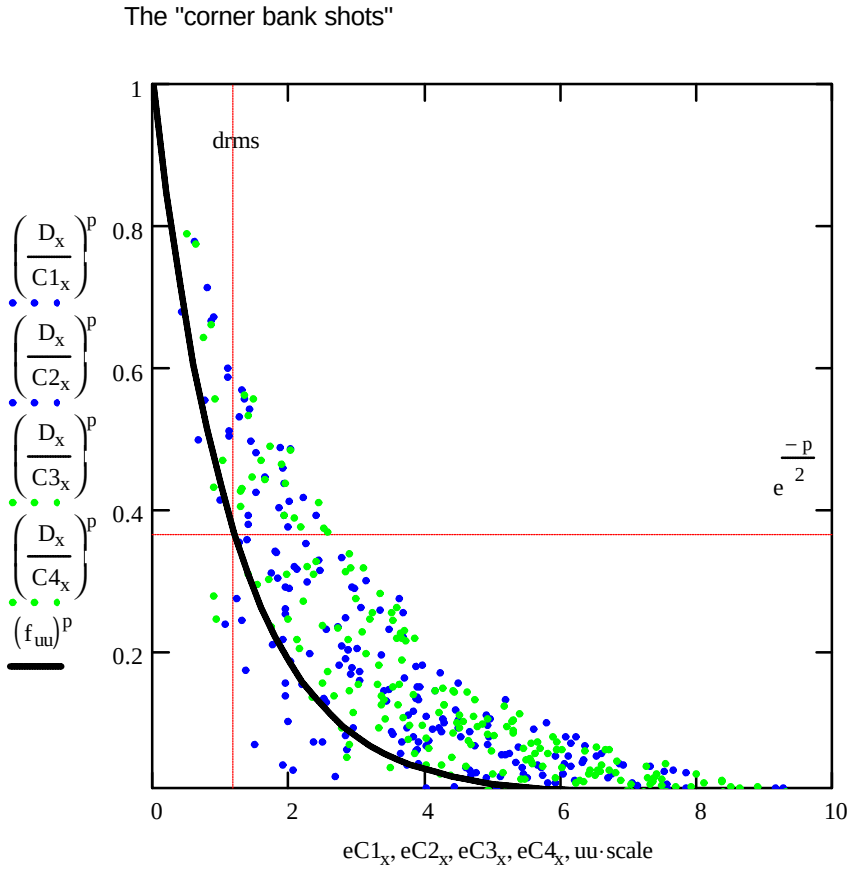

Figure 10. Energy delay profile vs. excess delay in m for all corner reflected components compared with exponential EDP.

An exponential EDP is not a very good fit to the room calculation. Since this case is deterministic, the actual 13-reflection room model can be used.

Arrange the various components for plotting a sample, and writing multipath data file:

$xs = 99 \qquad xs4 := \mathrm{floor}\left(\frac{xs}{4}\right) \qquad xs4 = 24 \qquad xx1 := 0..xs4$

$$Ref0_{xx1} := \left(\frac{D_{xx1}}{R1_{xx1}} \cdot \Gamma m\right) \qquad Ref1_{xx1} := \left(\frac{D_{xx1}}{R1_{xx1}} \cdot \Gamma_{2m}\right)$$

$$Ref0_{xx1+1+xs4} := \left(\frac{D_{xx1}}{R2_{xx1}} \cdot \Gamma m\right) \qquad Ref1_{xx1+1+xs4} := \left(\frac{D_{xx1}}{R2_{xx1}} \cdot \Gamma_{2m}\right)$$

$$Ref0_{xx1+(1+xs4)\cdot 2} := \left(\frac{D_{xx1}}{R3_{xx1}} \cdot \Gamma m\right) \qquad Ref1_{xx1+(1+xs4)\cdot 2} := \left(\frac{D_{xx1}}{R3_{xx1}} \cdot \Gamma_{2m}\right)$$

$$Ref0_{xx1+(1+xs4)\cdot 3} := \left(\frac{D_{xx1}}{R4_{xx1}} \cdot \Gamma m\right) \qquad Ref1_{xx1+(1+xs4)\cdot 3} := \left(\frac{D_{xx1}}{R4_{xx1}} \cdot \Gamma_{2m}\right)$$

$$Cor0_{xx1} := \left(\frac{D_{xx1}}{C1_{xx1}} \cdot \Gamma m^2\right) \qquad Cor0_{xx1+(1+xs4)\cdot 2} := \left(\frac{D_{xx1}}{C3_{xx1}} \cdot \Gamma m^2\right)$$

$$Cor0_{xx1+1+xs4} := \left(\frac{D_{xx1}}{C2_{xx1}} \cdot \Gamma m^2\right) \qquad Cor0_{xx1+(1+xs4)\cdot 3} := \left(\frac{D_{xx1}}{C4_{xx1}} \cdot \Gamma m^2\right)$$

$$Gnd_{xx1} := \left(\frac{D_{xx1}}{Gr_{xx1}} \cdot \Gamma m\right) \cdot \left(\frac{Dg_{xx1}}{Gr_{xx1}}\right)^2$$

Delays:

$$eRef1_{xx1+(1+xs4)\cdot 0} := eR1_{xx1} + eW \qquad eRef0_{xx1+(1+xs4)\cdot 0} := eR1_{xx1} \qquad eCor0_{xx1+(1+xs4)\cdot 0} := eC1_{xx1}$$

$$eRef1_{xx1+(1+xs4)\cdot 1} := eR2_{xx1} + eW \qquad eRef0_{xx1+(1+xs4)\cdot 1} := eR2_{xx1} \qquad eCor0_{xx1+(1+xs4)\cdot 1} := eC2_{xx1}$$

$$eRef1_{xx1+(1+xs4)\cdot 2} := eR3_{xx1} + eW \qquad eRef0_{xx1+(1+xs4)\cdot 2} := eR3_{xx1} \qquad eCor0_{xx1+(1+xs4)\cdot 2} := eC3_{xx1}$$

$$eRef1_{xx1+(1+xs4)\cdot 3} := eR4_{xx1} + eW \qquad eRef0_{xx1+(1+xs4)\cdot 3} := eR4_{xx1} \qquad eCor0_{xx1+(1+xs4)\cdot 3} := eC4_{xx1}$$

LOS, Case-1: 100 realizations data file. $NS := \frac{10^9}{c}$

Array of (X1,Y1,H1, X2,Y2,H2)

$WR_{x,0} := X1r_x \quad WR_{x,1} := Y1r_x \quad WR_{x,2} := H1_x \quad WR_{x,3} := X2r_x \quad WR_{x,4} := Y2r_x \quad WR_{x,5} := H2_x$

Array of primary wall reflections and their excess delays:

$$WR_{x,6} := \frac{D_x}{R1_x} \cdot \Gamma m \qquad WR_{x,8} := \frac{D_x}{R2_x} \cdot \Gamma m \qquad WR_{x,10} := \frac{D_x}{R3_x} \cdot \Gamma m \qquad WR_{x,12} := \frac{D_x}{R4_x} \cdot \Gamma m$$

$$WR_{x,7} := eR1_x \cdot NS \qquad WR_{x,9} := eR2_x \cdot NS \qquad WR_{x,11} := eR3_x \cdot NS \qquad WR_{x,13} := eR4_x \cdot NS$$

Array of corner reflections and their excess delays:

$$WR_{x,14} := \frac{D_x}{C1_x} \cdot \Gamma m^2 \qquad WR_{x,16} := \frac{D_x}{C2_x} \cdot \Gamma m^2 \qquad WR_{x,18} := \frac{D_x}{C3_x} \cdot \Gamma m^2 \qquad WR_{x,20} := \frac{D_x}{C4_x} \cdot \Gamma m^2$$

$$WR_{x,15} := eC1_x \cdot NS \qquad WR_{x,17} := eC2_x \cdot NS \qquad WR_{x,19} := eC3_x \cdot NS \qquad WR_{x,21} := eC4_x \cdot NS$$

Array of primary ground reflections and their excess delays:

$$WR_{x,22} := \left(\frac{D_x}{Gr_x} \cdot \Gamma m\right) \cdot \left(\frac{Dg_x}{Gr_x}\right)^2 \qquad WR_{x,23} := eG_x \cdot NS$$

Array of secondary wall reflections and their excess delays:

$$WR_{x,24} := \frac{D_x}{R1_x} \cdot \Gamma_{2m} \qquad WR_{x,26} := \frac{D_x}{R2_x} \cdot \Gamma_{2m}$$

$$WR_{x,25} := \left(eR1_x + eW\right) \cdot NS \qquad WR_{x,27} := \left(eR2_x + eW\right) \cdot NS$$

$$WR_{x,28} := \frac{D_x}{R3_x} \cdot \Gamma_{2m} \qquad WR_{x,30} := \frac{D_x}{R4_x} \cdot \Gamma_{2m}$$

$$WR_{x,29} := \left(eR3_x + eW\right) \cdot NS \qquad WR_{x,31} := \left(eR4_x + eW\right) \cdot NS$$

$rows(WR) = 100 \qquad cols(WR) = 32$

Generate data array: WRITEPRN("15-04-0505-04-004a-los_1000MHz.txt") := WR

File is 100 rows by 32 columns, each row is 32 numbers:
X1 Y1 H1 X2 Y2 H2 a1 d1 a2 d2 ... a13 d13 where the aX dX are amplitude-delay pairs

Energy of reflection components relative to their direct path energy. There are four distinct clusters of energy:
(1) Wall refelcted paths
(2) Corner refelections
(3) Wall reflections with double internal bounce
(4) Ground reflections

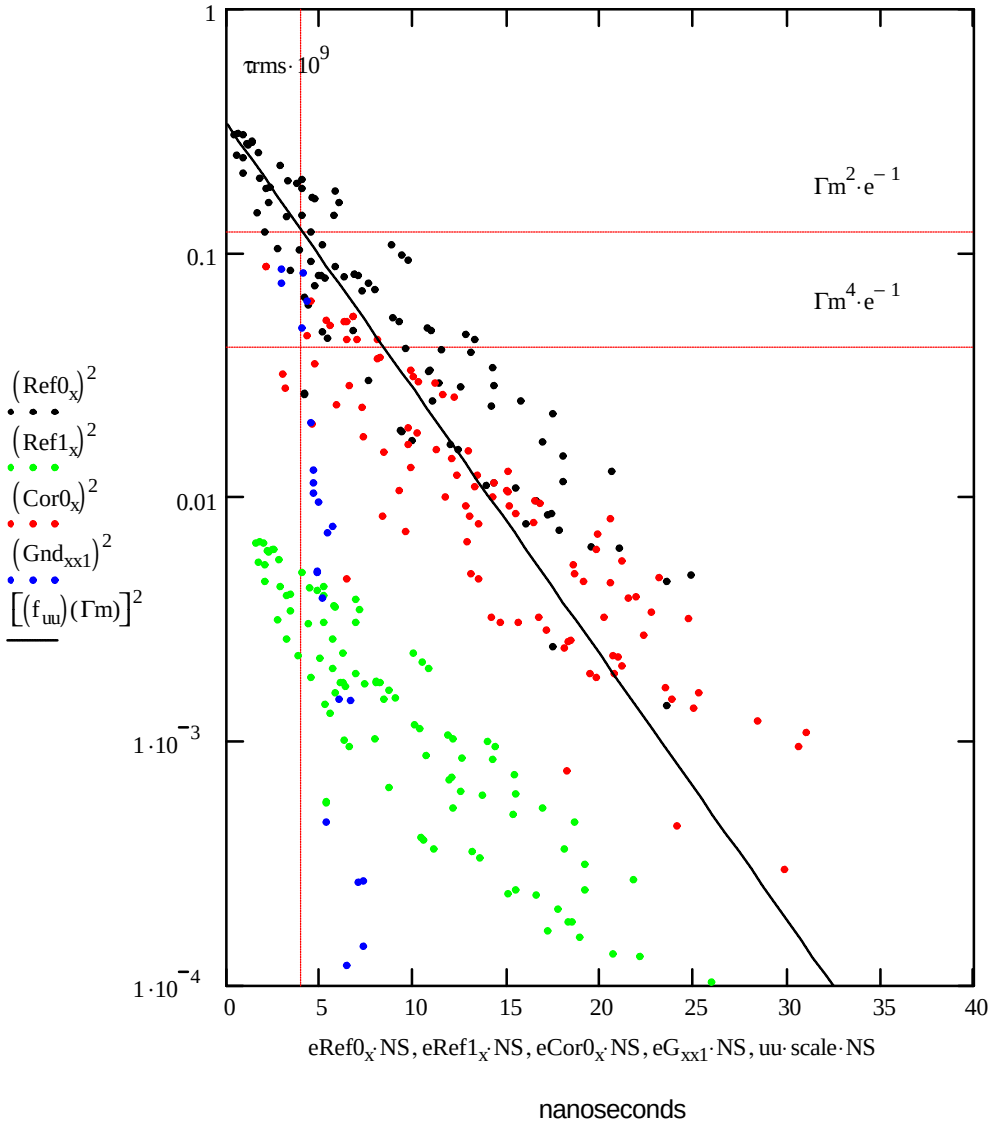

Figure 11. Multipath Energy vs. excess delay, m, for all components. Solid line represents an exponential distribution with the same delay spread.

A mean excess delay is found from

$$Delay_i := \frac{\left(eR1_i + eR2_i + eR3_i + eR4_i\right)\cdot(1 + eW) + eG_i \ldots + eC1_i + eC2_i + eC3_i + eC4_i}{13} \quad (21)$$

$Dmn := mean(Delay)$ $\quad Dmn = 2.345$ m

$median(Delay) = 2.357$ $\quad \frac{median(Delay)}{c}\cdot 10^9 = 7.862$ nanoseconds

The mean ray arrival interval Ts is derived form the mean excess delay.

$$Ts := \frac{Dmn}{c} \qquad Ts\cdot 10^9 = 7.822 \text{ nS} \quad (22)$$

We now have all the required components for the multipath portion of a channel model.

For the line of sight (LOS) model components, we have a direct path d, and wall reflected multipath components that carry energy in addition to the free space path between the transmitter and the receiver. The i-th realization of the in-room LOS channel impulse response field spectral density is thus:

$$\begin{aligned} H_{LOSi}(t) := {} & Vfs_i(d) + \Gamma m\cdot\left(\frac{Dg_i}{Gr_i}\right)\cdot Vfs(d + eG)\cdot\delta\left(t - \frac{eG}{c}\right)\ldots \\ & + \Gamma m\cdot\left(\begin{array}{l} Vfs_i(d + eR1)\cdot\delta\left(t - \frac{eR1}{c}\right)\ldots \\ + Vfs_i(d + eR2)\cdot\delta\left(t - \frac{eR2}{c}\right)\ldots \\ + Vfs_i(d + eR3)\cdot\delta\left(t - \frac{eR3}{c}\right)\ldots \\ + Vfs_i(d + eR4)\cdot\delta\left(t - \frac{eR4}{c}\right) \end{array}\right) + \Gamma m^2\cdot\left(\begin{array}{l} Vfs_i(d + eC1)\cdot\delta\left(t - \frac{eC1}{c}\right)\ldots \\ + Vfs_i(d + eC2)\cdot\delta\left(t - \frac{eC2}{c}\right)\ldots \\ + Vfs_i(d + eC3)\cdot\delta\left(t - \frac{eC3}{c}\right)\ldots \\ + Vfs_i(d + eC4)\cdot\delta\left(t - \frac{eC4}{c}\right) \end{array}\right)\ldots \\ & + \Gamma m\cdot(1 + \Gamma m)^2\cdot\left(\begin{array}{l} Vfs_i(d + eR1 + eW)\cdot\delta\left(t - \frac{eR1}{c} - \frac{eW}{c}\right)\ldots \\ + Vfs_i(d + eR2 + eW)\cdot\delta\left(t - \frac{eR2}{c} - \frac{eW}{c}\right)\ldots \\ + Vfs_i(d + eR3 + eW)\cdot\delta\left(t - \frac{eR3}{c} - \frac{eW}{c}\right)\ldots \\ + Vfs_i(d + eR4 + eW)\cdot\delta\left(t - \frac{eR4}{c} - \frac{eW}{c}\right) \end{array}\right) \end{aligned} \quad (23)$$

and equivalently $$H_{LOSi}(t) := Vfs_i(d)\cdot\left(\frac{d_i}{D_i} + \sum_{z=0}^{12} WR_{i,6+2\cdot z}\cdot\delta\left(t - WR_{i,7+2\cdot z}\right)\right) \quad (23a)$$

and the magnetic field strength spectral density at distance d is based on a spherical wave

$$Vfs(d) := \sqrt{\frac{\mu\cdot c}{4\pi}}\cdot\frac{1}{d} \quad \text{[corrected: rev 3].} \quad (24)$$

$m := 1$ The m-th realization; normalized to direct component

$ua := 1..4$

Ground component: $G00 := \left(\frac{D_m}{Gr_m}\cdot\Gamma m\right)\cdot\left(\frac{Dg_m}{Gr_m}\right)^2$

Wall reflected components, and their delays:

$R0_1 := \left(\frac{D_m}{R1_m}\cdot\Gamma m\right)$ $R0_2 := \left(\frac{D_m}{R2_m}\cdot\Gamma m\right)$ $R0_3 := \left(\frac{D_m}{R3_m}\cdot\Gamma m\right)$ $R0_4 := \left(\frac{D_m}{R4_m}\cdot\Gamma m\right)$

$eR00_1 := eR1_m\cdot NS$ $eR00_2 := eR2_m\cdot NS$ $eR00_3 := eR3_m\cdot NS$ $eR00_4 := eR4_m\cdot NS$

Secondary wall reflections, with bounce inside the wall, and their delays:

$R1_1 := \left(\frac{D_m}{R1_m + eW}\cdot\Gamma_{2m}\right)$ $R1_2 := \left(\frac{D_m}{R2_m}\cdot\Gamma_{2m}\right)$ $R1_3 := \left(\frac{D_m}{R3_m}\cdot\Gamma_{2m}\right)$ $R1_4 := \left(\frac{D_m}{R4_m}\cdot\Gamma_{2m}\right)$

$eR01_{ua} := eR00_{ua} + eW\cdot NS$

Corner reflected components and their delays:

$C0_1 := \left(\frac{D_m}{C1_m}\cdot\Gamma m^2\right)$ $C0_2 := \left(\frac{D_m}{C2_m}\cdot\Gamma m^2\right)$ $C0_3 := \left(\frac{D_m}{C3_m}\cdot\Gamma m^2\right)$ $C0_4 := \left(\frac{D_m}{C4_m}\cdot\Gamma m^2\right)$

$eC00_1 := eC1_m\cdot NS$ $eC00_2 := eC2_m\cdot NS$ $eC00_3 := eC3_m\cdot NS$ $eC00_4 := eC4_m\cdot NS$

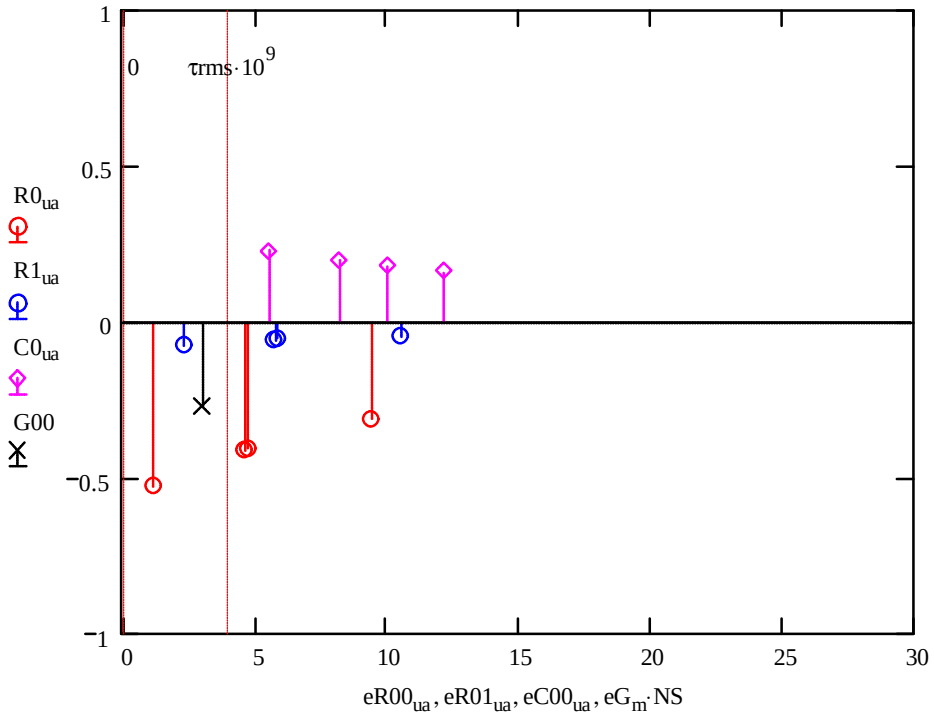

Figure 12. One particular realization of the LOS channel impulse amplitude response.

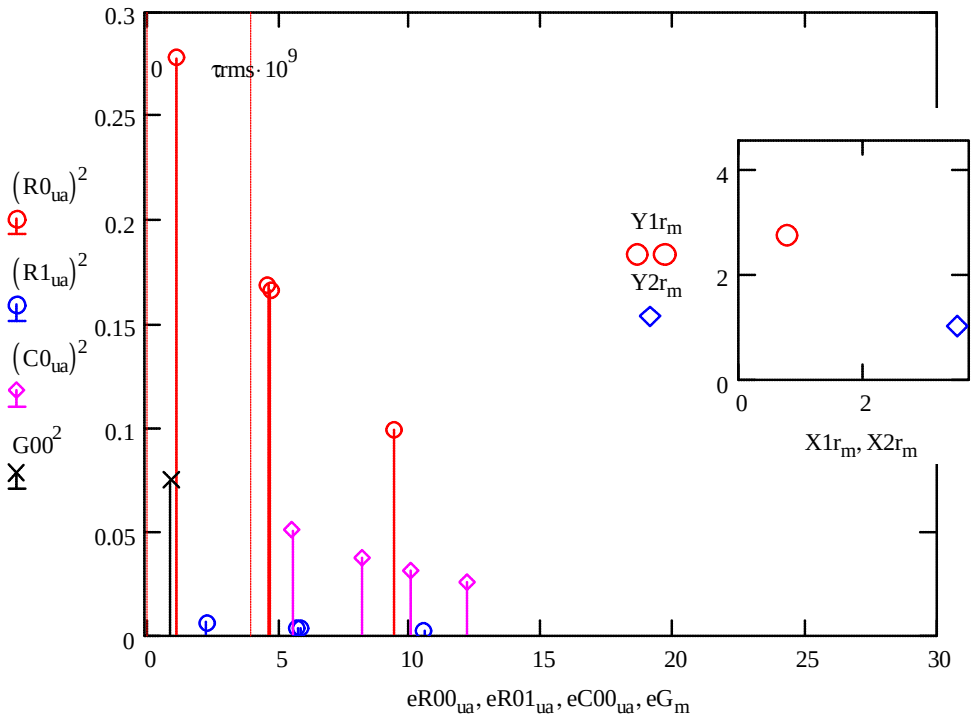

Figure 13. One particular realization of the LOS channel impulse energy response.

Plot the 100 realizations of the model:

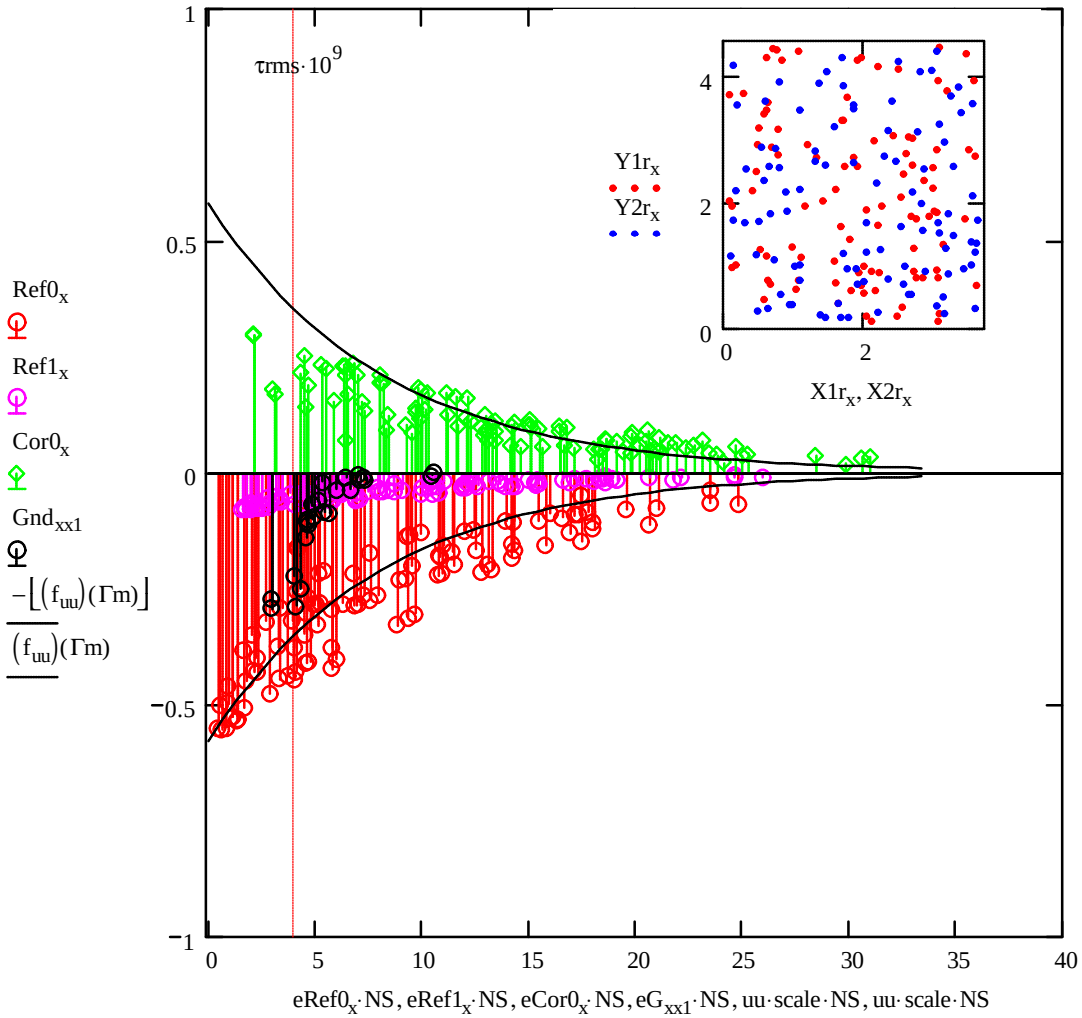

Figure 14. Hundred realizations of the LOS channel impulse amplitude responses.

The received energy by a "constant directivity" antenna aperture is:

$$Wrx := \frac{1.5}{4\cdot\pi}\cdot\frac{1}{f_2 - f_1}\cdot\left[\int_{f_1}^{f_2}\left(\frac{c}{f}\right)^2\cdot\eta_{ant}(f)\cdot EIRPsd(f)\,df\right] \quad (25)$$

where:

$\eta_{ant}(f)$ is the antenna efficiency as a function of frequency

$EIRPsd(f)$ is the radiated effective istropically radiated power spectral density

Thus the collected signal at the receiver is:

$$S(t) := H_{LOSi}(t)\cdot\sqrt{Wrx} \quad (26)$$

Signal S(t) contains all of the multipath components, weighted by the receiver antenna aperture, and by the receiver antenna efficiency. The method of signal detection, signal convolution the receiver filter, multiplication by the receiver template, and the signal processing will determine which and how many and how efficiently the multipath components are utilized.

The following parameters specific the UWB radio performance in a room-LOS condition:
(1) Room dimensions RoomX and RoomY, and minimum distance to a wall dt
(2) Antenna heights, between h1 and h2
(3) Radiated power spectral density EIRPsd(f)
(4) Receiver antenna aperture Ae
(5) Multipath signal profile S(t)
(6) Average reflection coefficient Γm

Derived parameters include:
- RMS delay spread τrms,
- the mean ray arrival rate Ts
- excess energy factor in the room is Wx

$\tau rms = 3.991\times 10^{-9}$ sec

$Ts = 7.822\times 10^{-9}$ sec

$Wx = 1.548$

Here:

$RoomX = 3.7$		m
$RoomY = 4.6$		m
$h1 = 1$	$h2 = 2$	m
$dt = 0.1$		m

Accounting for the total energy, the "excess" energy in the room Wx should approximately be balanced by the average wall-transmitted energy, thus: $10\log[(Wx)(1 + \Gamma m^2)]$ should approximately equal 0 dB.

$$10\cdot\log\left[\left(1-\Gamma m^2\right)\cdot Wx\right] = 0.116 \quad \text{dB} \quad (27)$$

A parametric study reveals that τrms is approximately the maximum propagation distance in the room, including maximum antenna height difference, multiplied by (0.2/c).

Case 2: Non-Line of Sight Multipath Model

The Jakes [Jakes 1974] model with exponential EDP will be applied, here for UWB pulses in non-line of sight (NLOS) cases. Thus the multipath impulses are exponentially distributed, their arrival interval is randomly distributed in windows of duration Ts.

Jakes Channel Model for f < 1000 MHz follows.

The mean ray Tm arrival interval is based on the LOS room model. A total of 13 paths with a mean delay of Ts were found. Thus the mean ray arrival interval is 2Ts/13:

$$Tm := Ts \cdot \frac{2}{13} \qquad Tm = 1.203 \times 10^{-9} \tag{28}$$

The maximum number of components considered is based on the largest delay spread. Here τmax = 55 ns.

$$\tau max := 55 \cdot 10^{-9}$$

$$Kmax := floor\left(5 \cdot \frac{\tau max}{Tm}\right) \qquad Kmax = 228 \qquad k := 0..Kmax - 1$$

The 100 multipath realizations of delays TM are randomly distributed in "bins" that are Tm wide and spaced Tm. TM is 100 rows (realizations) of Kmax columns.

$$TM := \left| \begin{array}{l} \text{for } r \in 0..99 \\ \quad \text{for } c \in 0, 1..Kmax - 1 \\ \quad\quad M_{r,c} \leftarrow c + rnd(1) \\ M \end{array} \right. \tag{29}$$

Channel coefficient hk is normally distributed with unity standard deviation:

$$hk := \left| \begin{array}{l} hk1 \leftarrow rnorm(Kmax \cdot 100, 0, 1) \\ \text{for } r \in 0..99 \\ \quad \text{for } c \in 0, 1..Kmax - 1 \\ \quad\quad M_{r,c} \leftarrow hk1_{(r+1)\cdot(c+1)-1} \\ M \end{array} \right. \tag{30}$$

$r := 0..\text{rows}(TM) - 1$ $co := 0..\text{cols}(TM) - 1$

$\text{rows}(TM) = 100$ $\text{cols}(TM) = 228$ $\text{rows}(hk) = 100$ $\text{cols}(hk) = 228$

(sanity check): $\text{mean}(hk) = -0.016$ $\text{stdev}(hk) = 1.014$

The random variable have now been established. The same set can be used for each distance realization.

A value for $\tau 0$ and Dt that approximately match channel models CM2, CM3, and CM4 in their appropriate distances [IEEE802 02/249], and [DaSilva 2003] is:

$\tau 0 := 4.5 \cdot 10^{-9}$ $Dt := 1$

Relationship between distance and delay spread is:

$$\tau rmsN(d, Dt, \tau 0) := \tau 0 \cdot \sqrt{\frac{d}{Dt}} \quad (31)$$

Multipath coefficients can be geenerated entirely from arrays $\sigma 1$ and hk along with the relationship between delay spread and distance, and the random time delay array TM.

WRITEPRN("15-04-0505-04-004a-NLOS_1000MHz_TM.txt") := TM

WRITEPRN("15-04-0505-04-004a-NLOS_1000MHz_HK.txt") := hk

$\text{rows}(hk) = 100$ $\text{cols}(hk) = 228$

File TM is 100 rows (realizations) by 228 columns of delay coefficients normalized to Tm.

File hk is 100 rows (realizations) by 228 columns of amplitude coefficients normalized at distance Dt.

Channel impulse responses are re-constructed and scaled for any distance d using:

Coefficients at d, m: $d := 5$ (example shown for d=5 m)

$$hd_{r,co} := \left(\sqrt{1 - \exp\left(\frac{-Tm}{\tau rmsN(d, Dt, \tau 0)}\right)}\right) \cdot hk_{r,co} \cdot \left(\exp\left(-\frac{Tm \cdot co}{2 \cdot \tau 0}\right)\right)^{\frac{\tau 0}{\tau rmsN(d, Dt, \tau 0)}} \quad (32)$$

Check coefficient energy: $NorM := \sqrt{\frac{1}{100} \cdot \left[\sum_r \left[\sum_{co} \left(\left|hd_{r,co}\right|\right)^2\right]\right]}$ $NorM = 1$

The corresponding time delay coefficients are: $Tm \cdot TM_{r,co}$

$$Umax := 50 \quad uu := 0..Umax \qquad tu_{uu} := \frac{uu}{Umax}\cdot 300\cdot nanosec$$

Comparison enevlope

$$theo_{uu} := \left[\left(1 - \exp\left(\frac{-Tm}{\tau rmsN(d, Dt, \tau 0)}\right)\right)\exp\left(-\frac{tu_{uu}}{\tau rmsN(d, Dt, \tau 0)}\right)\right]^{0.5}$$

Amplitude delay profile

$$d = 5 \qquad \tau rmsN(d, Dt, \tau 0)\cdot 10^{9} = 10.062$$

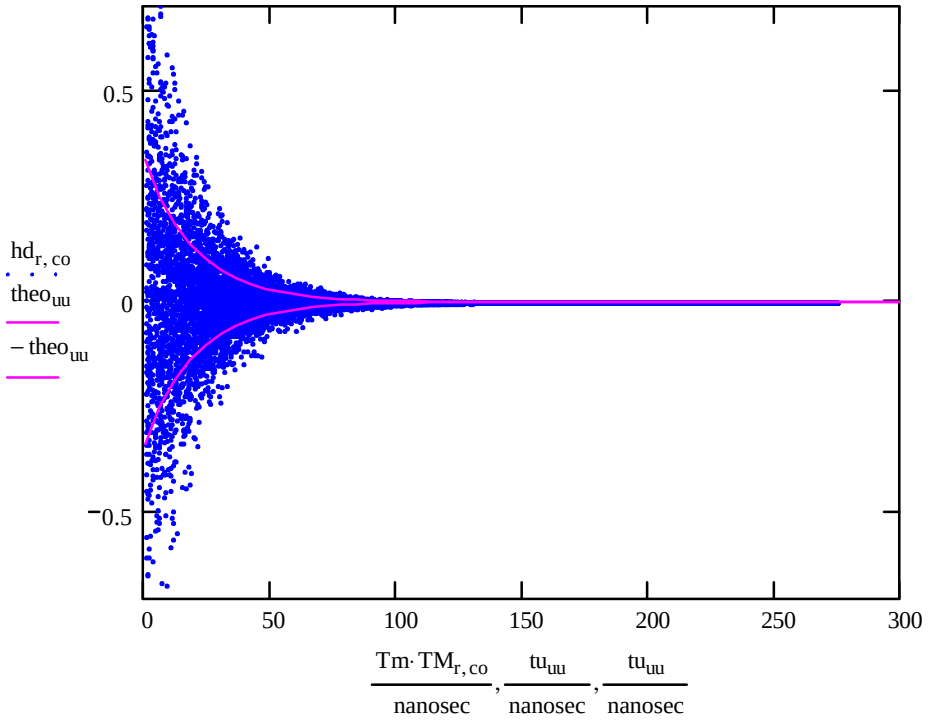

Figure 15. One Hundred realizations of the NLOS channel model at d=5 m.

Coefficients at d, m: $d := 20$ (example shown for d= 20 m)

$$th20_{uu} := \left[\left(1 - \exp\left(\frac{-Tm}{\tau rmsN(d, Dt, \tau 0)}\right)\right)\exp\left(-\frac{tu_{uu}}{\tau rmsN(d, Dt, \tau 0)}\right)\right]^{0.5}$$

$$hd20_{r,co} := \left(\sqrt{1 - \exp\left(\frac{-Tm}{\tau rmsN(d, Dt, \tau 0)}\right)}\right)\cdot hk_{r,co}\cdot\left(\exp\left(-\frac{Tm\cdot co}{2\cdot\tau 0}\right)\right)^{\frac{\tau 0}{\tau rmsN(d, Dt, \tau 0)}}$$

$d = 20$ $\tau rmsN(d, Dt, \tau 0)\cdot 10^{9} = 20.125$

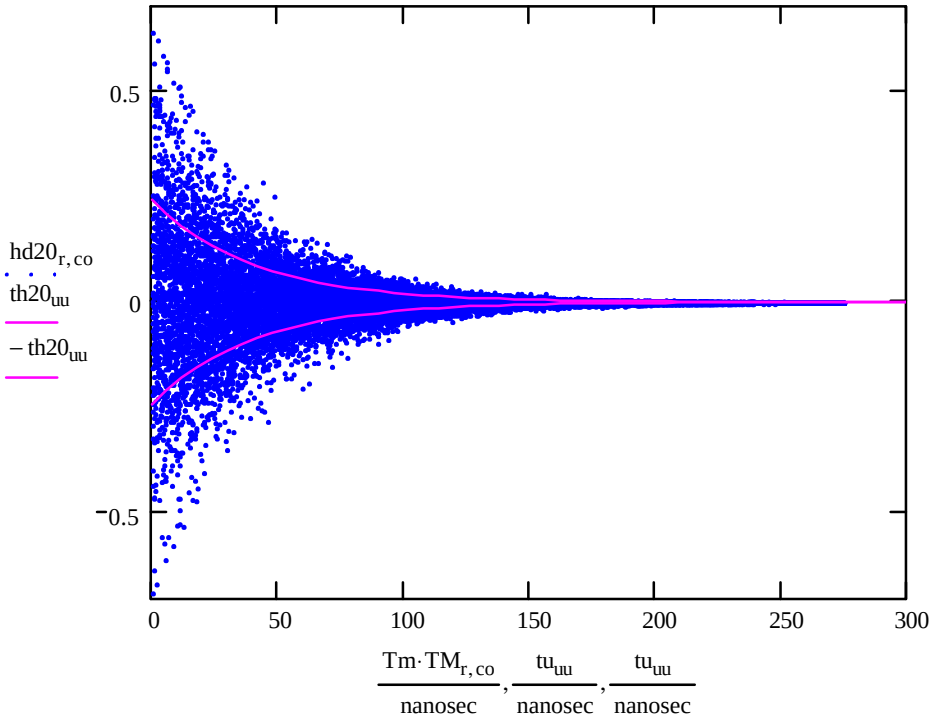

Figure 16. One Hundred realizations of the NLOS channel model at d=20 m.

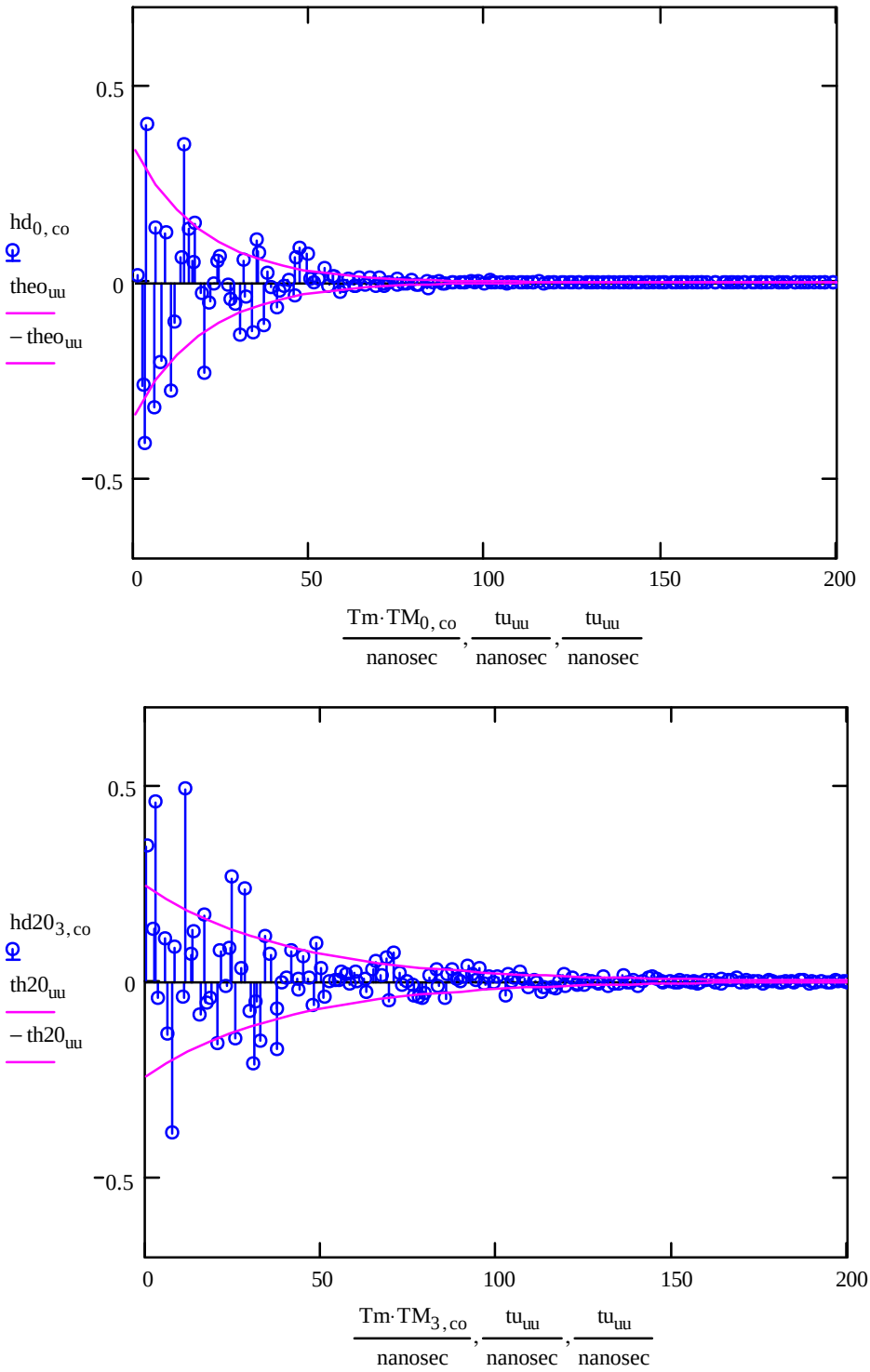

Figure 17. Two particlar realizations of the NLOS channel model at d=5 m (top), and d=20 m (bottom).

NLOS multipath model, the r-th realization:

$$H_{NLOS}(t)_r := Vfs(d)\cdot\sqrt{Kf}\cdot\delta(0) + \left(\sqrt{1-Kf}\right)\cdot\sum_{c=0}^{Kmax} hd_{r,c}\cdot\delta\left(t - Tm\cdot TM_{r,c}\right) \quad (33)$$

The received signal is given by equation (25). Thus the collected signal at the receiver is:

$$S_N(t) := HN_{NLOSi}(t)\cdot\sqrt{Wrx} \quad (34)$$

The delay spread parameter is a function of distance, [Siwiak 2003], and here is modeled by the square root of distance, see slide 34 of [IEEE802 04/504]. Thus, as seen in Equation (31),

$$\tau rmsN(d, Dt, \tau 0) := \tau 0\cdot\sqrt{\frac{d}{Dt}}$$

A value for $\tau 0$ and Dt that approximately match channel models CM2, CM3, and CM4 in their appropriate distances [IEEE802 02/249], and is consistent with [DaSilva 2003] is:

$\tau 0 = 4.5\times 10^{-9}$ $Dt := 1$

Thus

$\tau rmsN(2, Dt, \tau 0) = 6.364\times 10^{-9}$ $\tau rmsN(5, Dt, \tau 0) = 1.006\times 10^{-8}$

$\tau rmsN(7, Dt, \tau 0) = 1.191\times 10^{-8}$ $\tau rmsN(10, Dt, \tau 0) = 1.423\times 10^{-8}$

$\tau rmsN(20, Dt, \tau 0) = 2.012\times 10^{-8}$ $\tau rmsN(30, Dt, \tau 0) = 2.465\times 10^{-8}$

$\tau rmsN(50, Dt, \tau 0) = 3.182\times 10^{-8}$ $\tau rmsN(100, Dt, \tau 0) = 4.5\times 10^{-8}$

The choice of trms increasing as the squareroot of distance will result in an average power law behavior of approximately 2.5 for a receiver not employing a rake or channel equalization technique.

Signal SN(t) contains all of the multipath components, weighted by the receiver antenna aperture, and by the receiver antenna efficiency. The method of signal detection, signal convolution the receiver filter, multiplication by the receiver template, and the signal processing will determine which and how many and how efficiently the multipath components are utilized.

The following parameters specific the UWB radio performance in a N-LOS condition:
(1) RMS delay spread parameter $\tau 0$ s mulitplied by the square root of d/Dt
(2) Mean interval between rays Tm s
(3) Fraction of energy in direct ray Kf
(4) Radiated power spectral density EIRPsd(f)
(5) Receiver antenna aperture Ae
(6) Multipath signal profile SN(t)

The Ricean K factor and Kf are related by: Kf=K/(K+1), or equaivalently K=Kf/(1-Kf), where Kf takes on the range [0, 1] where correspondingly, K takes on the range [0, ∞].

Here: $\tau 0 = 4.5\times 10^{-9}$ nanosec

$\frac{Tm}{nanosec} = 1.203$ nanosec